Deficiency for endoglin in tumor vasculature weakens the endothelial barrier to metastatic dissemination

Charlotte Anderberg,[1] Sara I. Cunha,[1] Zhenhua Zhai,[2] Eliane Cortez,[1,3] Evangelia Pardali,[4,5] Jill R. Johnson,[1] Marcela Franco,[1] Marta Páez-Ribes,[7] Ross Cordiner,[2] Jonas Fuxe,[1] Bengt R. Johansson,[8,9] Marie-José Goumans,[6] Oriol Casanovas,[7] Peter ten Dijke,[4,5] Helen M. Arthur,[2] and Kristian Pietras[1,3]

[1]Department of Medical Biochemistry and Biophysics, Division of Vascular Biology, Karolinska Institutet, SE-171 77 Stockholm, Sweden
[2]Institute of Genetic Medicine, Centre for Life, Newcastle University, Newcastle NE1 3BZ, England, UK
[3]Department of Laboratory Medicine Malmö, Lund University Cancer Center, Lund University, SE-205 02 Malmö, Sweden
[4]Department of Molecular Cell Biology, [5]Centre for Biomedical Genetics, and [6]Department of Anatomy and Embryology, Leiden University Medical Center, 2300 RC Leiden, Netherlands
[7]Tumor Angiogenesis Group, Translational Research Laboratory, Catalan Institute of Oncology–IDIBELL, L'Hospitalet de Llobregat, 08908 Barcelona, Spain
[8]Department of Biochemistry and [9]Electron Microscopy Unit, Sahlgrenska Academy, University of Gothenburg, SE-405 30 Gothenburg, Sweden

Therapy-induced resistance remains a significant hurdle to achieve long-lasting responses and cures in cancer patients. We investigated the long-term consequences of genetically impaired angiogenesis by engineering multiple tumor models deprived of endoglin, a co-receptor for TGF-β in endothelial cells actively engaged in angiogenesis. Tumors from endoglin-deficient mice adapted to the weakened angiogenic response, and refractoriness to diminished endoglin signaling was accompanied by increased metastatic capability. Mechanistic studies in multiple mouse models of cancer revealed that deficiency for endoglin resulted in a tumor vasculature that displayed hallmarks of endothelial-to-mesenchymal transition, a process of previously unknown significance in cancer biology, but shown by us to be associated with a reduced capacity of the vasculature to avert tumor cell intra- and extravasation. Nevertheless, tumors deprived of endoglin exhibited a delayed onset of resistance to anti-VEGF (vascular endothelial growth factor) agents, illustrating the therapeutic utility of combinatorial targeting of multiple angiogenic pathways for the treatment of cancer.

CORRESPONDENCE
Kristian Pietras:
Kristian.Pietras@med.lu.se

Abbreviations used: EndMT, endothelial-to-mesenchymal transition; HHT, hereditary hemorrhagic telangiectasia; PNET, pancreatic neuroendocrine tumor; VEGF, vascular endothelial growth factor.

Efforts to achieve an effective cure against malignant diseases are commonly thwarted by the rapid emergence of therapy-resistant cancer cells that serve as the basis for resurgence of the tumor despite initial shrinkage. High hopes were placed on the development of antiangiogenic drugs, as it was thought that this class of agents would be inherently impervious to mechanisms of acquired resistance by means of targeting the nonmalignant and genetically stable tumor endothelial cells (Kerbel, 1991, 1997). However, the initial clinical experience with drugs selectively targeting the tumor neovasculature, such as bevacizumab, sunitinib, and sorafenib, has been sobering. Major clinical responses to these drugs, with targeting of the prototypical proangiogenic vascular endothelial growth factor (VEGF) as a common denominator, are rare, and the median prolongation of progression-free survival is typically 2–6 mo with minimal effect on overall survival

C. Anderberg, S.I. Cunha, and Z. Zhai contributed equally to this paper and are listed in alphabetical order.
P. ten Dijke, H.M. Arthur, and K. Pietras contributed equally to this paper.

The Rockefeller University Press $30.00
J. Exp. Med. 2013 Vol. 210 No. 3 563-579
www.jem.org/cgi/doi/10.1084/jem.20120662

after long-term follow up (Hurwitz et al., 2004; Escudier et al., 2007; Motzer et al., 2007). Mechanistic insight into evasive or intrinsic resistance to antiangiogenic therapy comes from recent preclinical trials (Bergers and Hanahan, 2008; Ebos et al., 2009b). Specifically, pharmacological inhibition of VEGF signaling in mouse models of cancer results in up-regulation of compensatory angiogenic pathways (Casanovas et al., 2005) and enhanced protective coverage of pericytes (Pietras and Hanahan, 2005). In parallel, tumors escalate the seeding of metastases as a result of hypoxia-induced increased local invasiveness (Ebos et al., 2009a; Pàez-Ribes et al., 2009). In yet other studies, contradictory results were presented demonstrating no association between anti-VEGF therapy and metastatic behavior (Chung et al., 2012; Singh et al., 2012; Welti et al., 2012). Clearly, in depth mechanistic studies are warranted to resolve the apparent controversies.

Members of the TGF-β family act pleiotropically on most, if not all, cell types in the body by engaging a heterotetrameric complex of type I and type II receptors (ten Dijke and Arthur, 2007; Massagué, 2008). Genetic targeting studies in mice provide ample evidence for a role of signaling by TGF-β ligands, receptors, and downstream mediators during developmental angiogenesis, although the precise mechanism remains unclear (David et al., 2009; Cunha and Pietras, 2011; van Meeteren et al., 2011). Moreover, pharmacological blocking of signaling by the endothelial cell–restricted type I receptor activin receptor-like kinase 1 (ALK1) inhibits tumor growth by impairing pathological angiogenesis (Cunha et al., 2010; Mitchell et al., 2010; Hu-Lowe et al., 2011). Signaling by ALK1 is complemented by the TGF-β co-receptor endoglin (ten Dijke et al., 2008; Pérez-Gómez et al., 2010; Nassiri et al., 2011). Endoglin (also known as CD105) is selectively expressed by endothelial cells actively engaged in vasculogenesis, angiogenesis, and inflammation and acts to promote endothelial cell proliferation, migration, and tube formation (Jonker and Arthur, 2002; Torsney et al., 2003; Lebrin et al., 2004; Jerkic et al., 2006). Germline mutations in the gene encoding endoglin are causative of the vascular syndrome hereditary hemorrhagic telangiectasia (HHT), characterized by arteriovenous malformations and frequent bleedings (Shovlin, 2010), a condition partially phenocopied by mice lacking a single copy of *Eng* (Bourdeau et al., 1999; Li et al., 1999; Arthur et al., 2000; Torsney et al., 2003) and more recently in mice with endothelial-specific endoglin depletion (Mahmoud et al., 2010). In tumors, endoglin is selectively up-regulated on endothelial cells (Westphal et al., 1993; Burrows et al., 1995; Miller et al., 1999; Bernabeu et al., 2009), and in many different tumor types, including breast, colon, and lung carcinoma, abundant expression of endoglin is a predictor of poor survival (Kumar et al., 1999; Takahashi et al., 2001b; Wikström et al., 2002; Charpin et al., 2004; Dales et al., 2004; Martone et al., 2005). Accordingly, partial genetic ablation or antibody targeting of endoglin delays tumor growth in mouse models of cancer through inhibition of angiogenesis (Seon et al., 1997; Takahashi et al., 2001a; Düwel et al., 2007; Seon et al., 2011). Collectively, endoglin appears as a valid therapeutic target for efforts to suppress tumor angiogenesis, but it is not known whether the long-term efficacy of such targeting would be limited by induction of adaptive mechanisms.

Here, we have delineated a novel mode of metastatic dissemination associated with tumors refractory to attenuated expression of endoglin. Deficiency for even a single copy of endoglin was characterized by an increased seeding of metastases caused by a weakened endothelial cell barrier to tumor cell intra- and extravasation. Strikingly, endoglin-deficient endothelial cells adapted a more mesenchymal phenotype consequential to enhanced signaling through the TGF-β type I receptor ALK5; increased endothelial-to-mesenchymal transition (EndMT) in the tumor vasculature thus constitutes a novel mechanism for metastatic dissemination.

RESULTS

Endoglin deficiency results in angiogenic adaptation and increased metastatic spread

To determine the impact of genetic ablation of endoglin in the tumor vasculature, we first devised a set of studies using the prototypical RIP1-Tag2 mouse model of multistep development of pancreatic neuroendocrine tumors (PNETs; Hanahan, 1985). Tumors of RIP1-Tag2 mice arise from the β-cells of the pancreatic islets of Langerhans consequential to expression of the SV40 large T-antigen under control of the insulin promoter. After hyperplasia, the β-cell islets go through sequential premalignant and angiogenic stages of tumorigenesis (prevalent at 8–10 wk of age) before developing into locally invasive and metastatic carcinomas (at 12 wk of age). Previous work has underscored the clinical applicability of the RIP1-Tag2 model by accurately predicting the efficacy of recently approved targeted agents against VEGF and mTOR signaling for PNET (Pàez-Ribes et al., 2009; Chiu et al., 2010; Raymond et al., 2011; Yao et al., 2011).

First, we characterized the mRNA expression of endoglin in normal, hyperplastic, angiogenic, and tumorous pancreatic islets. Endoglin exhibited a peak of expression during the onset of angiogenesis, implying a functional role in the transition from hyperplastic to angiogenic lesions (Fig. 1 a). The expression of endoglin, as assessed by immunostaining, was confined to endothelial cells in the actively proliferating neovasculature of malignant lesions and not evident in pericytes or tumor cells (Fig. 1, b and c). Next, we made use of mice deficient for one copy of the endoglin gene ($Eng^{+/-}$) to analyze the impact of loss of endoglin in the context of PNET development. In agreement with the expression profile of endoglin, RIP1-Tag2;$Eng^{+/-}$ mice presented with fewer angiogenic islets at 9 wk of age, as identified under a stereological microscope (RIP1-Tag2;$Eng^{+/-}$ mice [$n = 6$], 8 ± 1.3 vs. RIP1-Tag2;$Eng^{+/+}$ mice [$n = 7$], 14.5 ± 2.9; $P < 0.0001$). The number of angiogenic islets of 12-wk-old RIP1-Tag2;$Eng^{+/-}$ mice was similarly reduced by 46% compared with RIP1-Tag2;$Eng^{+/+}$ littermates (Fig. 2 a). Isolation of angiogenic islets by gradient centrifugation confirmed that

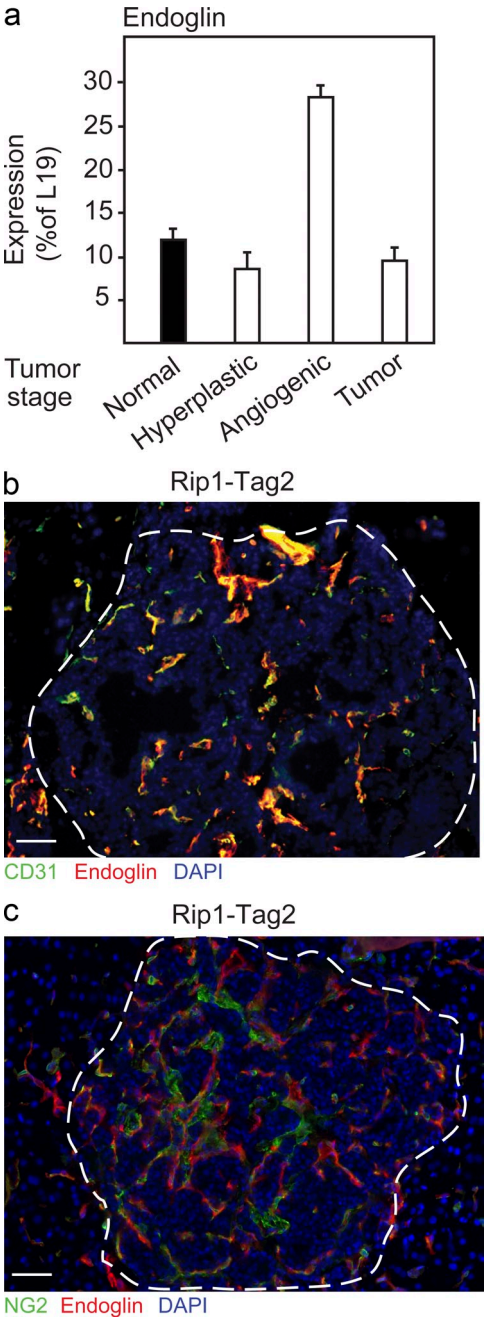

Figure 1. Endoglin is expressed by endothelial cells during the angiogenic switch of PNET in RIP1-Tag2 mice. (a) Quantitative RT-PCR analysis of expression of endoglin during the different stages of tumorigenic conversion in RIP1-Tag2 mice (a pool of material each derived from >10 mice was used for the analysis). Error bars depict SD. (b) Immunostaining for CD31 and endoglin in PNET lesion from RIP1-Tag2 mice. (c) Immunostaining for the pericyte marker NG2 and endoglin in PNET lesion from RIP1-Tag2 mice. (b and c) Cell nuclei are shown with DAPI. The dashed line marks the tumor-exocrine pancreas boundary. Bars, 50 µm.

endoglin-deficient RIP1-Tag2 mice harbored a reduced proportion of angiogenic versus hyperplastic islets at 12 wk of age (RIP1-Tag2;$Eng^{+/-}$ mice, 30% vs. RIP1-Tag2;$Eng^{+/+}$ mice, 56%; $P < 0.01$, χ^2-test). Moreover, the blockade in transition of neoplastic lesions to the angiogenic phase translated into a reduction of the number of overt tumors in mice partially deficient for endoglin (Fig. 2 b). In further support of an obstruction in the transition of pre-angiogenic lesions into tumors, 14/55 (25.5%) RIP1-Tag2;$Eng^{+/-}$ mice presented without any tumors, whereas only 1/22 (4.5%; $P < 0.05$, χ^2-test) littermate control mice were tumor free. Nevertheless, the mean total tumor volume per mouse was not different between the groups (Fig. 2 c), indicating that a majority of the RIP1-Tag2;$Eng^{+/-}$ mice eventually adapted to the initial impairment in tripping the angiogenic switch. No compensatory up-regulation of endoglin mRNA or protein in endothelial cells or other cell types was apparent in end-stage tumors from endoglin-deficient mice (unpublished data), suggesting alternative evasive action by tumors harboring a genetically stunted ability to initiate the angiogenic phase in the absence of endoglin.

Endoglin-deficient RIP1-Tag2 mice present with an increased number of hepatic metastases

Next, we sought to characterize the impact of blunted endoglin expression on the angiogenic and invasive program of PNET from RIP1-Tag2 mice. The vascular density of tumors and premalignant angiogenic lesions assessed by immunostaining for the luminal vessel marker podocalyxin (Horvat et al., 1986) was similar in PNET regardless of endoglin status (Fig. 2, d and e). Furthermore, the functionality of the end-stage tumor vessels, inferred by study of the degree of perfusion using fluorescein-coupled tomato lectin, was found to be unaffected by partial deficiency for endoglin in tumors (Fig. 2, f and g). The emergence of tumors resistant to treatment with VEGFR-blocking agents is characterized by increased metastatic spread consequential to a highly locally invasive phenotype (Casanovas et al., 2005; Pàez-Ribes et al., 2009). Having documented that ablation of endoglin also gives rise to an adaptive response, we wanted to investigate whether evasive action against genetically impaired angiogenesis also resulted in increased metastatic dissemination. The liver is the most frequent site for metastatic colonization of PNET in human patients (Pavel et al., 2012). Strikingly, RIP1-Tag2;$Eng^{+/-}$ mice presented with a threefold increased incidence of micrometastases expressing SV40 T-Ag embedded in the liver parenchyma, as compared with RIP1-Tag2;$Eng^{+/+}$ littermates (Fig. 2, h and i).

Increased metastatic spread in endoglin-deficient mice is an endothelial cell–autonomous event

To investigate whether tumor adaptation to genetic targeting of endoglin is an endothelial cell–autonomous event, we induced conditional ablation of both copies of the gene encoding endoglin specifically in endothelial cells through the use of tamoxifen injection of compound Eng^{iKOe} mice ($Eng^{fl/fl}$; Cdh5-Cre^{ERT2}; Mahmoud et al., 2010). Injection of the mouse lung carcinoma cell line LLC in Eng^{iKOe} mice resulted in an initial delay in the establishment of tumors compared with tamoxifen-treated control $Eng^{fl/fl}$ mice (day 6;

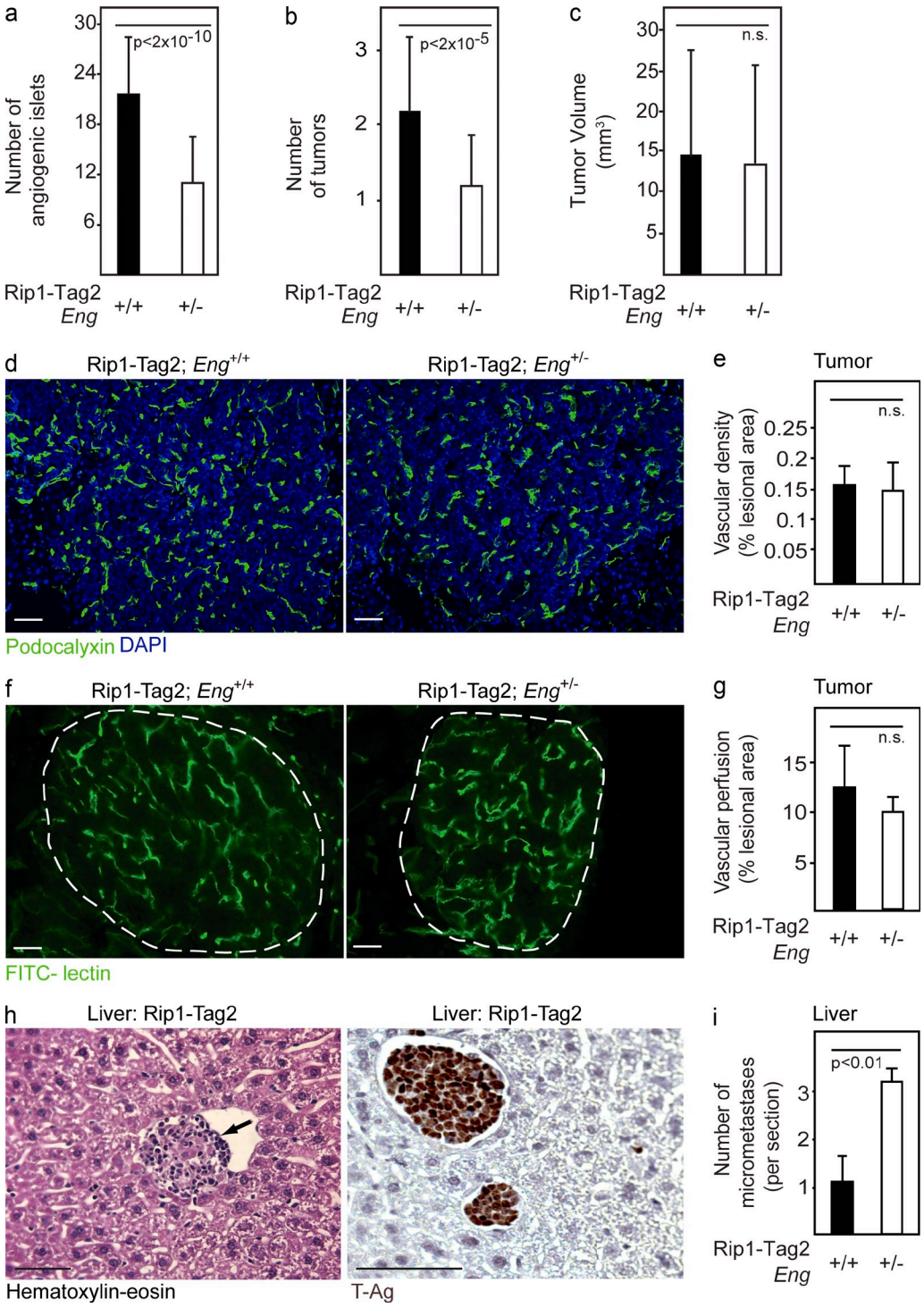

Figure 2. Increased metastatic seeding of tumors in endoglin-deficient mice. (a–c) Quantification of number of angiogenic islets (a), number of tumors (b), and total tumor burden (c) in 12-wk-old RIP1-Tag2;*Eng*$^{+/+}$ (n = 22) and RIP1-Tag2;*Eng*$^{+/-}$ mice (n = 55). (d and e) Immunostaining (d) and quantification (e) of total positively stained area for the vascular marker podocalyxin in PNETs from RIP1-Tag2;*Eng*$^{+/+}$ and RIP1-Tag2;*Eng*$^{+/-}$ mice. Analysis was performed using at least five mice per group. (f and g) Perfused vessels in PNETs from RIP1-Tag2;*Eng*$^{+/+}$ and RIP1-Tag2;*Eng*$^{+/-}$ mice visualized (f) and quantified (g) by fluorescein-labeled tomato lectin. The dashed line marks the tumor-exocrine pancreas boundary. Analysis was performed using three mice per group. (d and f) Cell nuclei are shown with DAPI. (h) Representative picture of hematoxylin-eosin staining (left) and immunostaining for SV40 T-antigen (T-Ag; right) of a micrometastatic liver lesion. The arrow inside the sinusoidal vessel marks metastatic lesion. (i) Quantification of micrometastatic foci in the liver of RIP1-Tag2;*Eng*$^{+/+}$ and RIP1-Tag2;*Eng*$^{+/-}$ mice at 12 wk of age. Error bars depict SD; n.s., not significantly different. Bars, 50 µm.

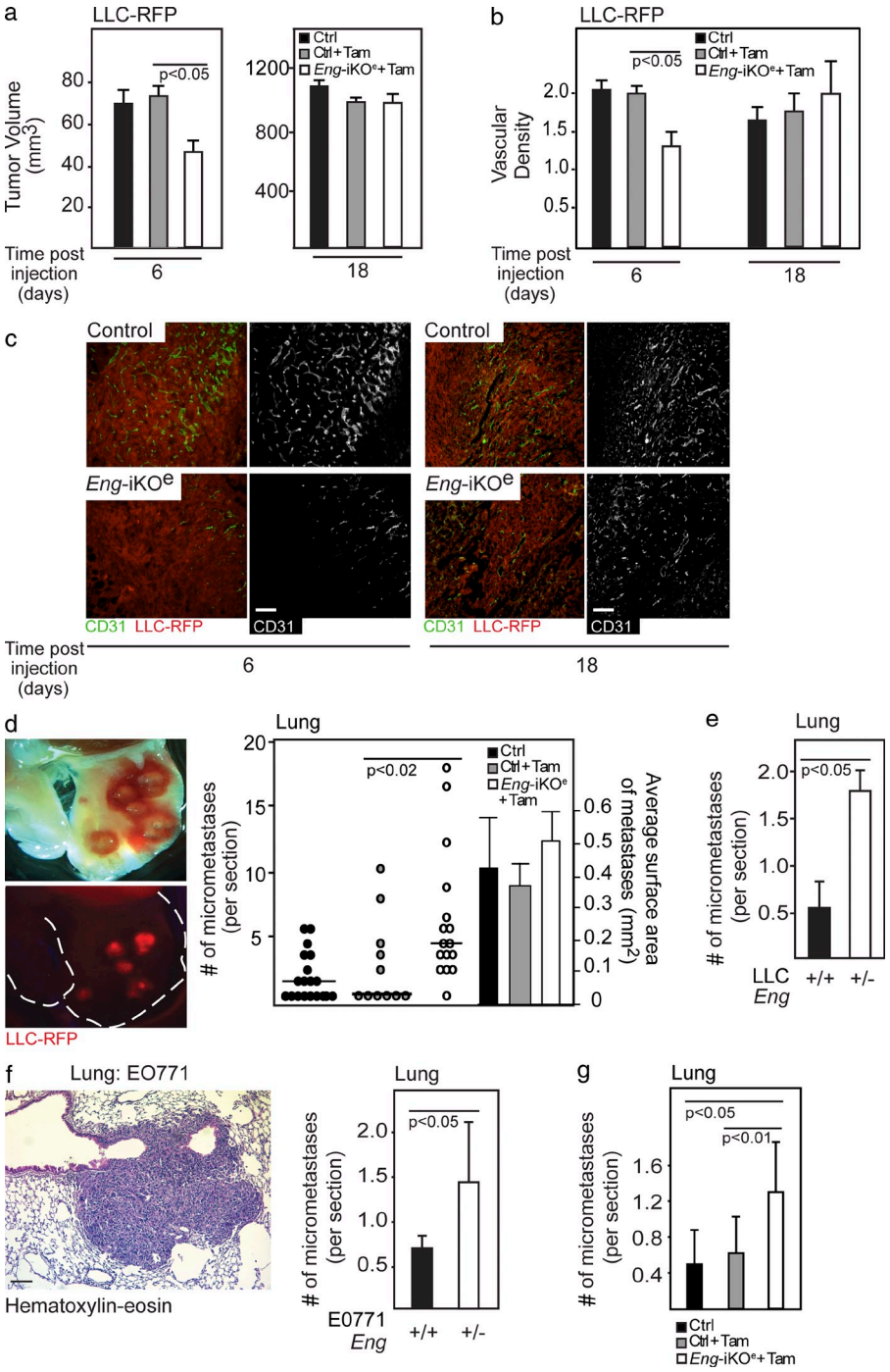

Figure 3. Increased metastatic seeding in endoglin-deficient mice is an endothelial cell–autonomous event. (a) In vivo tumor volume of subcutaneously injected LLC-RFP cells at 6 and 18 d in control (n = 7 and n = 19, respectively), tamoxifen-treated control (n = 7 and n = 11, respectively), and Eng^{iKOe} (n = 9 and n = 15, respectively) mice. (b and c) Quantification (b) and immunostaining (c) of vessel density of LLC-RFP tumors using CD31 during initial phases of tumor development and at the endpoint of the experiment in control (n = 7 and n = 19, respectively), tamoxifen-treated controls (n = 7 and n = 11, respectively), and Eng^{iKOe} (n = 9 and n = 15, respectively) mice. (d) Representative picture and quantification of lung metastases using fluorescent imaging of RFP-tagged LLC cells (LLC-RFP) in control (n = 19), tamoxifen-treated control (n = 11) or Eng^{iKOe} (n = 15) mice with established subcutaneous tumors. A subset of mice (n = 8, 6, and 6, respectively) was also analyzed for the mean size of metastatic lesions. The horizontal lines represent median. Statistical analysis was performed using the Mann-Whitney U test. (e) Quantification of lung metastases of LLC-RFP tumors established subcutaneously in $Eng^{+/+}$ (n = 11) or $Eng^{+/-}$ (n = 9) mice. (f) Representative picture of hematoxylin-eosin staining of a micrometastatic lung lesion from EO771 tumors. Quantification of micrometastatic foci in the lung of EO771-bearing $Eng^{+/+}$ (n = 5) and $Eng^{+/-}$ (n = 5) mice. (g) Quantification of lung metastases from EO771 tumors established subcutaneously in control (n = 8), tamoxifen-treated control (Tam; n = 8), or Eng^{iKOe} (n = 8) mice. Error bars depict SD. Bars, 50 µm.

Fig. 3 a), in agreement with previous studies (Düwel et al., 2007). However, similar to the retardation of PNET development in RIP1-Tag2 mice, LLC tumors in Eng^{iKOe} mice eventually caught up, and at the conclusion of the experiment, tumor volume was indistinguishable from that of tumors in the control groups (day 18; Fig. 3 a). Consistently, the delay in establishment of LLC-RFP tumors in Eng^{iKOe} mice was mirrored in an initial, but transient, impediment to activate tumor vascularization in Eng^{iKOe} mice (Fig. 3, b and c). Tumors grown in Eng^{iKOe} mice were confirmed by immunostaining to lack endoglin expression (unpublished data). To further support the association between deficiency for endoglin and increased metastatic spread, we assessed the occurrence of lung metastases of LLC tumors grown in the Eng^{iKOe} mice. Indeed, mice with an induced endothelial cell–specific knockout of endoglin presented with a mean of threefold more metastatic foci in the lung than WT mice (Fig. 3 d). The mean size of the metastatic lesions did not differ significantly between the genotypes, indicating that metastatic seeding, rather than growth rate, was affected in

endoglin-deficient mice (Fig. 3 d). LLC tumors injected subcutaneously into $Eng^{+/-}$ mice similarly gave rise to a significantly higher number of lung metastases than tumors grown in WT littermates, despite exhibiting a comparable growth rate (Fig. 3 e and not depicted).

To investigate the generality of the increased metastatic spread in tumors grown in endoglin-deficient mice, we established mouse mammary tumors by orthotopic implantation of EO771 cells (Casey et al., 1951) into the inguinal fat pad of $Eng^{+/-}$ mice or WT littermates. EO771 tumors were intrinsically resistant to the lowered expression of endoglin in terms of growth rate and vascular density (unpublished data). In contrast, lung metastases originating from EO771 tumors were 2.1-fold more prevalent in $Eng^{+/-}$ mice compared with $Eng^{+/+}$ mice (Fig. 3 f). In further support, the frequency of lung metastases originating from EO771 tumors injected orthotopically into the mammary fat pad of Eng^{iKOe} mice was significantly increased compared with littermate control mice (Fig. 3 g), with no apparent effect observed on the primary tumor growth or vascular density at the end of the experiment (not depicted). Collectively, data from five different mouse models of cancer representing three distinct malignant diseases demonstrate that a reduced gene dosage of endoglin in endothelial cells provokes the outgrowth of tumors with an increased propensity to seed distant metastases.

Endoglin heterozygosity maintains tumors in a sensitive state to VEGF inhibition

The compound tumor phenotype observed in mice with loss of endoglin expression is remarkably similar to that observed in preclinical studies for tumors resistant to anti-VEGF therapy. Although the expression level of VEGF pathway members was not altered in angiogenic islets or tumors from endoglin-deficient RIP1-Tag2 mice (unpublished data), pharmacological or genetic targeting of endoglin interferes with VEGF-induced angiogenesis, indicating cross talk on a molecular level (unpublished data; Castonguay et al., 2011). Therefore, we decided to evaluate the effect of the absence of endoglin on VEGF-blunted neovascularization. First, we treated RIP1-Tag2;$Eng^{+/+}$ and RIP1-Tag2;$Eng^{+/-}$ mice with the selective VEGFR tyrosine kinase inhibitor AG-028262 (Zou, H.Y. et al. 2004. Annual Meeting of the American Association for Cancer Research. Abstr. 2578). AG-028262 effectively blocked PNET growth in the RIP1-Tag2 tumor model when supplied in preventive short-term trials (unpublished data). However, in agreement with earlier studies (Casanovas et al., 2005; Pàez-Ribes et al., 2009), long-term therapy of RIP1-Tag2 mice with VEGF-blocking agents was not effective because of the emergence of refractory tumors supporting increased metastatic dissemination to the liver (Fig. 4, a and b). In striking contrast, PNETs of RIP1-Tag2;$Eng^{+/-}$ mice maintained sensitivity to AG-028262, as assessed by tumor size and vessel density, even during prolonged therapy (Fig. 4, a and c). Importantly, metastatic colonization of the liver was not increased after administration of AG-028262 to endoglin-deficient mice, indicating that reduced endoglin signaling counteracted the more malignant phenotype of tumor cells from mice treated with anti-VEGF therapy (Fig. 4 b). To determine whether the synergy between endoglin deficiency and AG-028262 was a direct effect of inhibition of VEGF signaling, we made use of the VEGFR2-neutralizing antibody DC101. Similar to our earlier observations, RIP1-Tag2;$Eng^{+/-}$ mice maintained sensitivity toward DC101, both in terms of delayed tumor growth and metastatic dissemination (Fig. 4, a and b).

The findings in the RIP1-Tag2 model were validated by the fact that EO771 tumors grown orthotopically in the mammary fat pad of $Eng^{+/-}$ mice had a similarly heightened sensitivity to anti-VEGF therapy and a concomitantly lowered incidence of lung metastases and decreased vascular density after AG-028262 therapy, compared with WT littermates (Fig. 4, d and e; and not depicted). Likewise, Eng^{iKOe} mice carrying subcutaneous LLC tumors presented with a dramatically reduced size of metastatic lesions in the lung compared with control mice after treatment with AG-028262, despite exhibiting similar growth rates (Fig. 4, f and g; and not depicted). Thus, concurrent attenuation of endoglin- and VEGF-induced signaling provided effective and long-term control of metastatic dissemination.

Endoglin deficiency leads to facilitated tumor cell intravasation

We sought to determine the mechanism for the increased propensity for hematogenous spread of tumors in endoglin-deficient mice. No significant difference was found in the incidence of locally invasive tumors between PNETs from RIP1-Tag2;$Eng^{+/+}$ and RIP1-Tag2;$Eng^{+/-}$ mice as assessed by histopathological scoring (unpublished data). In addition, no endoglin-dependent hypoxia or alterations in the tumor-wide expression of >40 genes involved in the metastatic or angiogenic program of tumors were noted, as assessed by pimonidazole adduct formation (unpublished data) and by analysis of global gene expression (unpublished data), respectively. Next, with the purpose of evaluating whether endothelial cells with diminished endoglin expression are permissive to tumor cell transmigration to a greater extent than their WT counterparts, we established an in vitro transwell assay. An endothelial cell line stably expressing a short hairpin RNA targeting endoglin (bEnd3.1/shEng) was seeded onto membranes in trans-well inserts and allowed to form a monolayer. Next, prelabeled βTC-3 tumor cells derived from a PNET of a RIP1-Tag2 mouse (Efrat et al., 1988) or EO771 cells were seeded on top of the endothelial cells, and malignant cell transmigration through the endothelial cell layer to the lower chamber was scored as a proxy for tumor cell intra-/extravasation. Compared with endothelial cells harboring a control vector, bEnd3.1/shEng allowed significantly more tumor cells to pass through the endothelial cell layer, indicating that endoglin is important for maintaining the integrity of the endothelial cell barrier (Fig. 5 a). Likewise, 4-OH-tamoxifen–induced knockout of endoglin from microvascular lung endothelial cells isolated from $Eng^{fl/fl}$; Rosa26-Cre^{ERT} mice carrying the

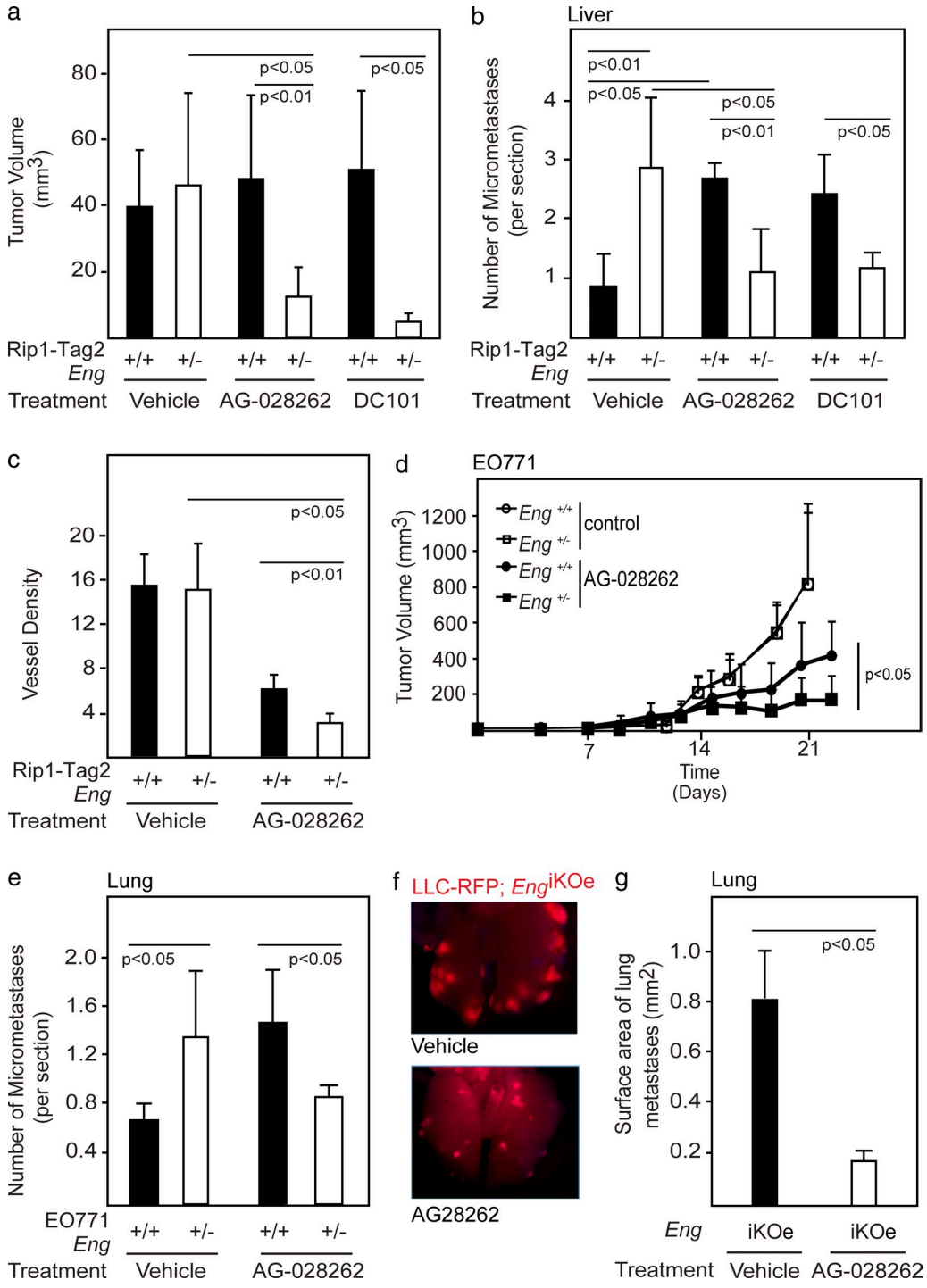

Figure 4. Endoglin deficiency maintains tumors in a sensitive state to VEGF inhibition. (a) Total tumor burden of RIP1-Tag2;*Eng*$^{+/+}$ and RIP1-Tag2;*Eng*$^{+/-}$ mice at 13 wk of age after 3 wk of treatment with vehicle (n = 6 and n = 5, respectively), the small molecule VEGFR inhibitor AG-028262 (n = 9 and n = 5, respectively), or the VEGFR2-neutralizing antibody DC101 (n = 3 in each group). The data shown are representative of two independent experiments. (b) Quantification of micrometastatic PNET foci in the liver of RIP1-Tag2;*Eng*$^{+/+}$ and RIP1-Tag2;*Eng*$^{+/-}$ mice at 13 wk of age after 3 wk of treatment with vehicle (n = 4 in each group), AG-028262 (n = 4 in each group), or DC101 (n = 3 in each group). (c) Quantification of total positively stained area for the vascular marker podocalyxin in PNET from RIP1-Tag2;*Eng*$^{+/+}$ and RIP1-Tag2;*Eng*$^{+/-}$ mice after 3 wk treatment with vehicle or AG-028262. (d and e) In vivo growth rate (d) and quantification of micrometastatic lung foci (e) of orthotopically implanted EO771 mammary tumors in *Eng*$^{+/+}$ and *Eng*$^{+/-}$ mice during treatment with control or AG-028262 (n = 5–11). Data from control mice are reproduced from Fig. 3 f to allow easy comparison. (f and g) Representative image (f) and quantification (g) of metastatic foci of LLC-RFP tumors in the lungs of *Eng*^{iK0e} mice treated with vehicle or AG-028262. Error bars depict SD.

Immortomouse transgene facilitated transmigration of LLC-RFP cells across an endothelial monolayer, compared with parental, noninduced cells (termed MLEC;$Eng^{-/-}$ and MLEC; $Eng^{+/+}$, respectively; Fig. 5 a).

The observed increased colonization of metastases in endoglin-deficient mice can be causal to an improved seeding of tumor cells from the primary site into the circulation, a facilitated extravasation of tumor cells into the metastatic site, or both. To distinguish between these possibilities, we assessed the number of circulating malignant cells, as well as the propensity of intravenously injected tumor cells to extravasate in endoglin-deficient mice. We found that whole blood of RIP1-Tag2;$Eng^{+/-}$ mice contained a 57% higher abundance of the transgenic transcript for SV40 T-Ag than RIP1-Tag2;$Eng^{+/+}$ mice, suggesting that an increased number of tumor cells were seeded into the circulation of endoglin-deficient mice by primary PNETs (Fig. 5 b). Ultrastructural analysis of tumor capillaries from RIP1-Tag2 mice demonstrated no gross differences in the architecture of the vessels or overt malformations in endothelial cell junctions in endoglin-deficient mice, suggesting that the increased abundance of tumor cells in the circulation of RIP1-Tag2;$Eng^{+/-}$ mice was the result of a regulated process and not simply of a physical loss of endothelial barrier patency (Fig. 5 c). In keeping with this proposition, the tumor vasculature in RIP1-Tag2;$Eng^{+/-}$ mice was found neither to be leakier to fluorescently labeled small molecules (1 kD cadaverine) or macromolecules (70 kD dextran; Fig. 5 d and not depicted) nor to exhibit a decreased perfusion grade (Fig. 2, f and g). Likewise, no difference in leakiness to dextran was observed in the vasculature of lungs of Eng^{iKOe} mice after induction of endoglin deficiency (unpublished data).

No increased transmigration of tumor cells into the liver was found after intravenous injection of prelabeled βTC-3 cells into nontumor-bearing endoglin-deficient mice, consistent with the negligible level of endoglin expression by liver sinusoids (Fig. 5, e and f; and not depicted). In contrast, when LLC tumor cells were introduced into the blood stream of Eng^{iKOe} mice, 13-fold more metastatic foci were found in the lungs 2 wk later compared with control mice, indicating that in this tumor model the endoglin-deficient vasculature was defective in its ability to contain tumor cells in the lung circulation (Fig. 5 g and not depicted). Notably, lung capillaries were found to readily express endoglin in WT mice (Fig. 5 f). Thus, augmented metastatic colonization in endoglin-deficient mice was found to be consequential to an increased endothelial cell leniency toward malignant cell intra- and/or extravasation, indicative of a role for endoglin in regulating cellular transmigration across the endothelial barrier.

Facilitated tumor cell intravasation is accompanied by EndMT in endoglin-deficient tumors

To gain insight into the underlying cause of the facilitated transmigration of tumor cells across the endoglin-deficient endothelial cell barrier, we investigated the junctional integrity of the tumor vasculature using immunostaining for CD31. In PNETs from WT RIP1-Tag2 mice, CD31 was robustly expressed by endothelial cells of both large vessels and small neo-angiogenic capillaries and sprouts (Fig. 6 a). Partial loss of endoglin in RIP1-Tag2;$Eng^{+/-}$ mice resulted in a considerable decrease of strongly $CD31^+$ small capillaries in PNETs (Fig. 6, a and b). Double immunostaining for the endothelial cell marker podocalyxin and CD31 revealed that small caliber $podocalyxin^+$ vessels of tumors from RIP1-Tag2;$Eng^{+/-}$ mice were only weakly expressing CD31 (Fig. 6 c). Endoglin-deficient endothelial cells that retained close to normal protein levels of CD31 exhibited a more diffuse localization of CD31 and were partially detached from the $podocalyxin^+$ endothelial cells (Fig. 6 d), in agreement with an earlier study describing the phenotype of endothelial progenitor cells undergoing TGF-β–mediated EndMT (Moonen et al., 2010). EndMT, a process of hitherto unknown functional importance in tumors, involves loss of endothelial marker expression, such as CD31, concomitant with an increase in mesenchymal marker expression, such as α–smooth muscle actin (α-SMA; Zeisberg et al., 2007). To investigate whether endothelial cells adopted a more mesenchymal state in endoglin-deficient tumors, we performed immunostaining for α-SMA. Indeed, RIP1-Tag2;$Eng^{+/-}$ mice presented with PNETs with an increase of vessel-associated $\alpha\text{-SMA}^+$ cells (Fig. 6 e and not depicted). Furthermore, a subset of vessels appeared composed of cells co-expressing the endothelial cell marker podocalyxin and the mesenchymal marker α-SMA, indicative of ongoing EndMT (Fig. 6 e and not depicted). High-power confocal microscopy also revealed diminution and redistribution of CD31 into a more diffuse localization in endothelial cells, accompanied by an increased abundance of α-SMA immunoreactivity inside or juxtaposed to the endothelium in PNETs from RIP1-Tag2;$Eng^{+/-}$ mice (Fig. 6 f and not depicted). The vasculature of RIP1-Tag2;$Eng^{+/-}$ mice was further invested by an increased number of cells expressing the mural cell marker NG2 (Fig. 6 g) Likewise, the vasculature of EO771 tumors grown in $Eng^{+/-}$ mice were invested with a 2.2-fold higher abundance of cells expressing mesenchymal markers such as α-SMA, cells which to a large extent also co-expressed the endothelial cell marker podocalyxin (Fig. 6, h and i). Thus, $Eng^{+/-}$ mice present with a subset of malignant lesions exhibiting a vasculature composed of cells with a mixed endothelial and mesenchymal identity.

Endoglin-deficient tumor endothelial cells express Twist and are more prone to undergo EndMT

In seeking additional evidence for the manifestation of EndMT in endoglin-deficient endothelial cells in vivo, we isolated tumor endothelial cells from RIP1-Tag2 mice. Our analyses demonstrated a dramatically increased content of the mRNA for Twist, a transcriptional regulator known to be a key activator of EndMT, in isolated endothelial cells from tumors of RIP1-Tag2;$Eng^{+/-}$ mice, compared with tumors from WT littermates (Fig. 7 a). The up-regulation of Twist in endoglin-deficient endothelial cells was evident neither in liver endothelial cells nor in nonendothelial cells of tumors

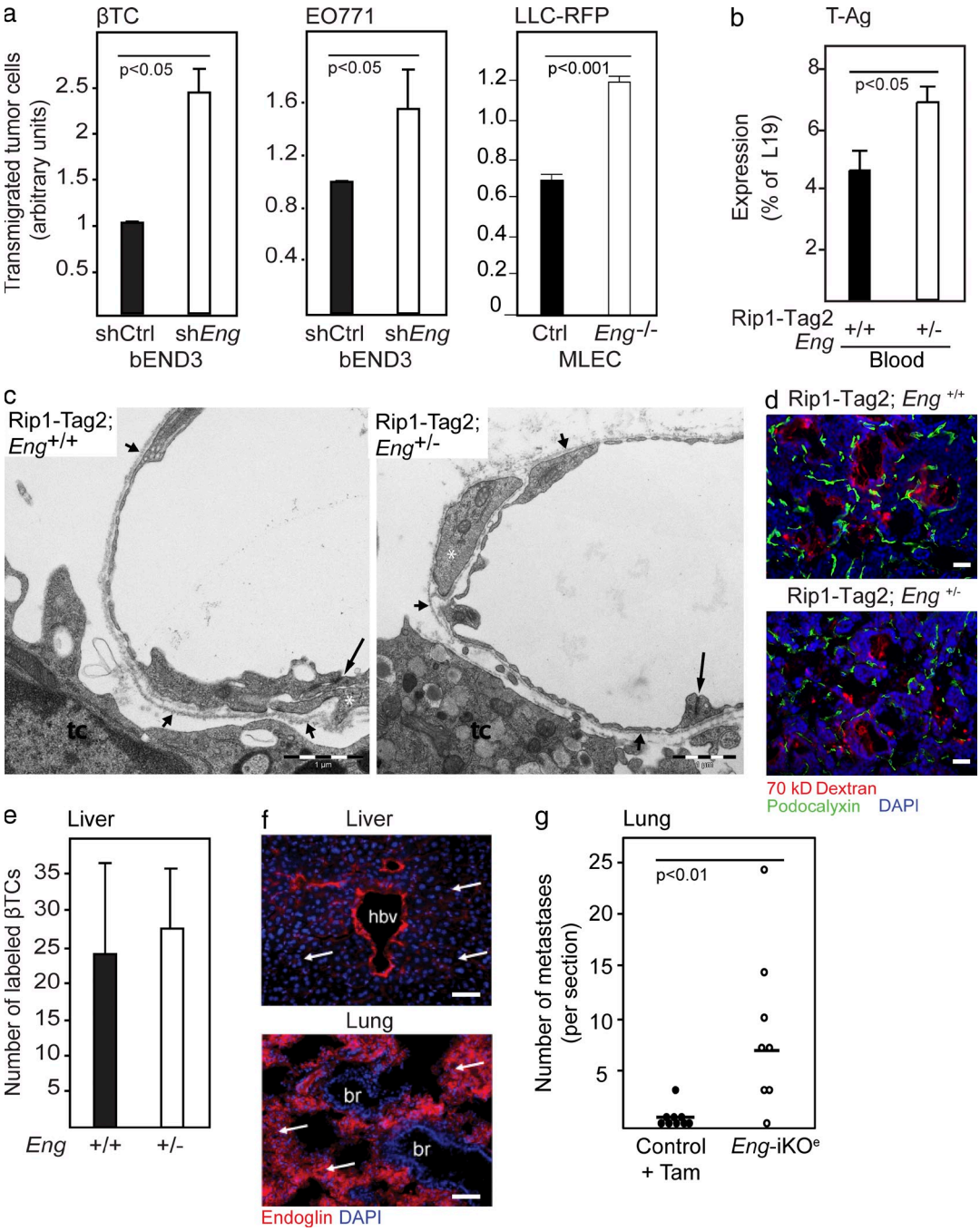

Figure 5. The increased metastatic seeding in endoglin-deficient mice is a result of disruption of the endothelial cell barrier. (a) Transmigration of βTC-3 cells derived from a PNET in a RIP1-Tag2 mouse, EO771 cells, or LLC-RFP cells through a monolayer of bEnd3.1 endothelial cells expressing either shRNA-endoglin or control vector or through a monolayer of primary mouse lung endothelial cells isolated from Eng^{iKOe} mice carrying the Immortomouse transgene (MLEC). The mean of two to three independent experiments is shown. (b) Quantitative RT-PCR detection of SV40 T-Ag transcripts in whole blood from RIP1-Tag2;$Eng^{+/+}$ (n = 10) and RIP1-Tag2;$Eng^{+/-}$ (n = 5) mice. (c) Electron micrographic views of transversely cut tumor microvessels in RIP1-Tag2;$Eng^{+/+}$ and RIP1-Tag2;$Eng^{+/-}$ mice. Interendothelial junctions are indicated from the luminal aspect (long arrows). Continuous periendothelial basal laminae (short arrows) invest cytoplasmic strands of pericytes (white asterisks). tc, tumor cell. (d) Detection of extravasated fluorescently labeled 70 kD dextran and immunostaining for podocalyxin of PNETs from RIP1-Tag2;$Eng^{+/+}$ mice and RIP1-Tag2;$Eng^{+/-}$ excised 4 min after injection of dextran. (e) Quantification of extravasated βTC-3 cell labeled with a fluorescent tracer (green) in the liver parenchyma from $Eng^{+/+}$ (n = 4) and $Eng^{+/-}$ (n = 3) mice 24 h after tail vein injection. (f) Immunohistochemical detection of endoglin in liver sinusoidal endothelial cells and lung capillaries. Cell nuclei are shown with DAPI. Arrows point out sinusoidal and lung capillaries. hbv, hepatic blood vessel; br, bronchiolus. (g) Quantification of LLC-RFP metastatic foci in the lung 15 d after tail vein injection in WT tamoxifen-treated (n = 9) and Eng^{iKOe} (n = 8). Horizontal lines represent median. Statistical analysis was performed using the Mann-Whitney U test. Error bars depict SD. Bars: (c) 1 µm; (d and f) 50 µm.

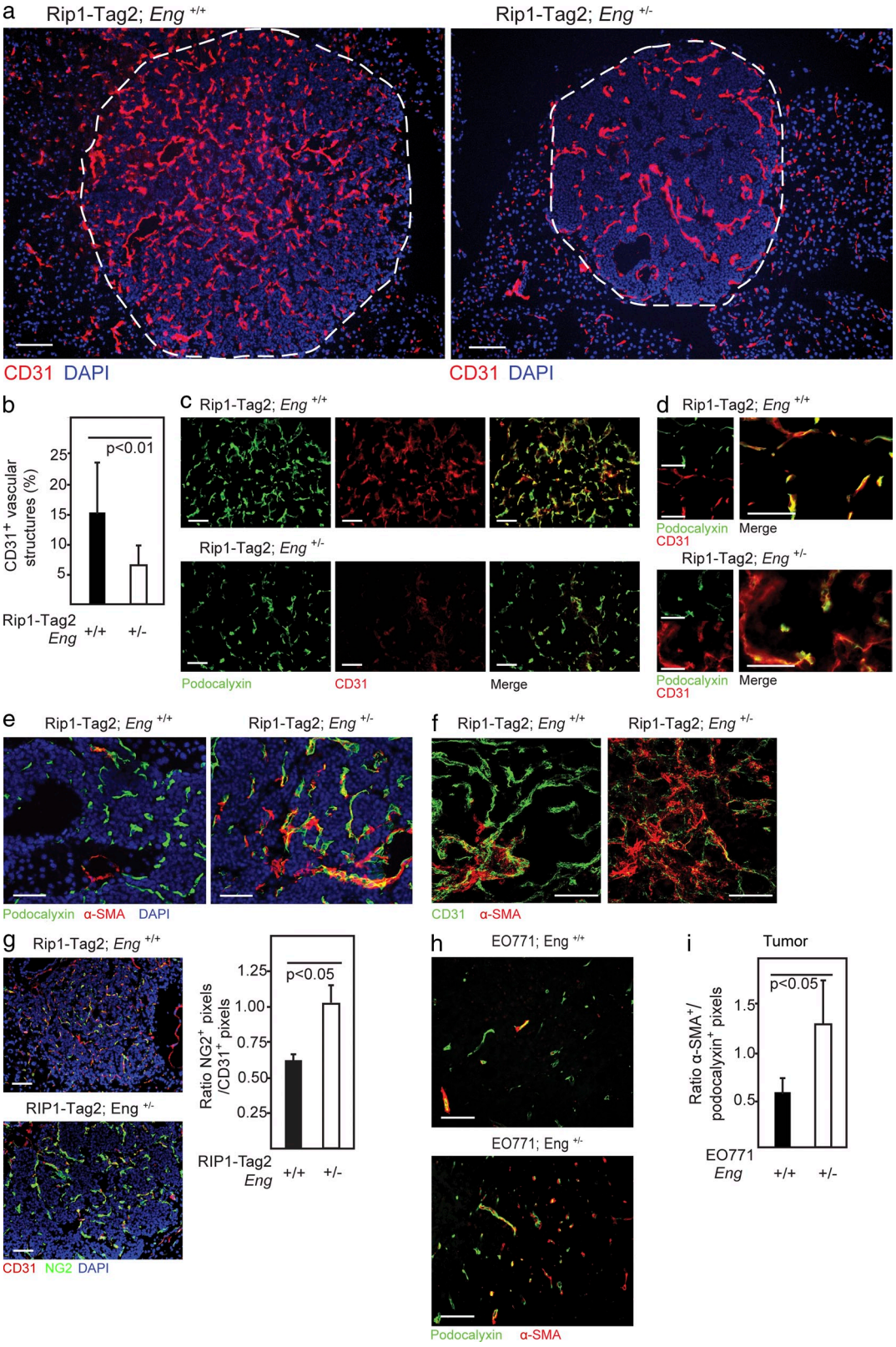

Figure 6. Reduced endoglin expression gives rise to hallmarks of EndMT in tumors in vivo. (a) Immunostaining for CD31 of PNETs from 12-wk-old RIP1-Tag2;*Eng*$^{+/+}$ and RIP1-Tag2;*Eng*$^{+/-}$ mice. The dashed line marks the tumor-exocrine pancreas boundary. (b) Quantification of vessels with high CD31 expression in PNET lesions from RIP1-Tag2;*Eng*$^{+/+}$ ($n = 3$) and RIP1-Tag2;*Eng*$^{+/-}$ ($n = 4$) mice. (c and d) Immunostaining for podocalyxin and CD31 of PNET lesions from 12-wk-old RIP1-Tag2;*Eng*$^{+/+}$ and RIP1-Tag2;*Eng*$^{+/-}$ mice. (e) Immunostaining for podocalyxin and α-SMA of PNET lesions from RIP1-Tag2;*Eng*$^{+/+}$

from RIP1-Tag2 mice, indicating that induction of EndMT is a specific trait of the PNET endothelium after genetic ablation of endoglin (Fig. 7 a and not depicted). Stimulation with TGF-β readily induced EndMT in endothelial cells in vitro, as indicated by a morphological switch from the typical cobblestone appearance of endothelial cells into an elongated and spindle-like shape (Fig. 7 b). To investigate whether loss of endoglin expression was sufficient to activate the program for EndMT, we again made use of the bEnd3.1/shEng cells with a diminished endoglin protein expression. Knockdown of endoglin resulted in an increased sensitivity of endothelial cells to undergo EndMT both at baseline conditions or after stimulation with TGF-β, as indicated by loss of CD31 and gain of α-SMA protein (Fig. 7, c and d). In contrast, inhibition of VEGF signaling by DC101 did not affect TGF-β–induced EndMT (unpublished data). In further support of the proposition that endoglin deficiency facilitated induction of EndMT, MLEC;$Eng^{-/-}$ cells exhibited an elongated morphology compared with MLEC;$Eng^{+/+}$ cells (unpublished data). Stable knockdown of Twist using lentiviral delivery of shRNA in MLEC;$Eng^{+/+}$ or MLEC;$Eng^{-/-}$ cells prevented TGF-β–induced EndMT (unpublished data), indicating a pivotal role for Twist as a downstream mediator of EndMT in the endoglin-deficient state. Twist knockdown in MLEC;$Eng^{-/-}$ cells also normalized the rate of transendothelial migration of βTC-3 cells (Fig. 7 e), indicating that Twist-induced EndMT of endoglin-deficient cells is underlying the defect in cellular barrier properties. Moreover, EndMT induced by TGF-β stimulation of MS1 pancreatic islet endothelial cells resulted in a greatly facilitated transmigration of βTC-3 cells (Fig. 7 f), strengthening the proposition that induction of TGF-β–mediated EndMT is paralleled by a weakened endothelial cell barrier to tumor cell transmigration. Knockdown of CD31 proved sufficient to enhance transendothelial tumor cell migration by either βTC-3 or EO771 cells (unpublished data), suggesting that the EndMT and consequential redistribution/reduced abundance of CD31 facilitated cellular transfer across the endothelium. To understand the molecular mechanism behind the observed EndMT in endoglin-deficient tumor vessels, we probed signaling downstream of the TGF-β type I receptor ALK5 in isolated PNET endothelial cells. ALK5 signaling is known to mediate EndMT (Medici et al., 2010; Moonen et al., 2010; Egorova et al., 2011) and to be antagonized by the action of endoglin (Lebrin et al., 2004; Blanco et al., 2005). In agreement with these previous studies, loss of one copy of the endoglin gene resulted in improved transcriptional activation of prototypical ALK5 target genes in vivo in endothelial cells isolated from PNETs of RIP1-Tag2;$Eng^{+/-}$ mice (Fig. 7 g), indicative of a molecular contribution of ALK5 to the EndMT. Indeed, the selective TGF-β type I receptor inhibitor LY364947 normalized the endothelial barrier properties of MLEC;$Eng^{-/-}$ cells (Fig. 7 g). In summary, consequential to reduced expression of endoglin, tumor endothelial cells up-regulate Twist and other ALK5 target genes, leading to EndMT and facilitated tumor cell transfer across the endothelial barrier.

DISCUSSION

The functional importance of EndMT in tumors has until now not been well understood. Our study identifies EndMT as a novel enabling factor for metastatic dissemination by facilitating tumor cell intra- and/or extravasation. Thus, in addition to promoting metastatic spread by direct stimulation of epithelial-to-mesenchymal transition of tumor cells (Padua and Massagué, 2009), TGF-β acts to assist transmigration of malignant cells across the endothelial cell barrier by inducing EndMT. In the context of metastatic dissemination, efforts to find therapeutic targets to reduce the spread of tumors have mostly focused on targeting the invasive properties of the malignant cell by searching for genetic alterations driving the progression of cancer into a systemic disease (Nguyen et al., 2009). Here, the properties of endothelial cells are highlighted as important tumor cell nonautonomous regulators of metastatic dissemination. It may be that genetic or molecular signaling events promoted by the cross talk between the tumor and the stroma interact to create a confined milieu favoring metastatic dissemination; such events may prove difficult to uncover using global analyses of tumor materials. Thus, further studies should aim at identifying local regulators of EndMT and tumor endothelial cell barrier properties to develop drugs that promote sealing of the intrinsic vascular barricade to prevent cancer spread.

The accelerated transition of endothelial cells with an engineered low expression of endoglin into a mesenchymal state, and the increased appearance of cells expressing α-SMA and NG2 as constituents of blood vessels in tumors deficient for endoglin, suggest that EndMT may also give rise to pericyte-like cells within tumors (Franco et al., 2011b). The aberrant occurrence of α-SMA$^+$ perivascular cells has been noted previously in conjunction with increased metastatic formation in RIP1-Tag2 mice deficient for a single or both copies of the gene encoding neural cell adhesion molecule (NCAM; Xian et al., 2006), raising the question of whether diminished expression of NCAM is part of the EndMT phenotype. Furthermore, we and others have recently identified an increased profusion of perivascular cells expressing α-SMA as a particular feature of a subset of tumors that are refractory to anti-VEGF therapy in mouse models of PNET and malignant melanoma, respectively (Helfrich et al., 2010; Franco et al., 2011a), although it was not investigated whether EndMT was

and RIP1-Tag2;$Eng^{+/-}$ mice. (f) Representative confocal micrograph of immunostaining for CD31 and α-SMA of PNET lesion from 12-wk-old RIP1-Tag2;$Eng^{+/+}$ and RIP1-Tag2;$Eng^{+/-}$ mice. (g) Immunostaining and quantification of NG2 and CD31 of sections of PNET from 12-wk-old RIP1-Tag2 mice. (a, e, and g) Cell nuclei are shown with DAPI. (h) Immunostaining for podocalyxin and α-SMA of EO771 tumors grown in $Eng^{+/+}$ or $Eng^{+/-}$ mice.(i) Quantification of α-SMA$^+$ vessels in EO771 tumors from $Eng^{+/+}$ ($n = 4$) and $Eng^{+/-}$ ($n = 4$) mice. Error bars depict SD. Bars: (a) Bars, 100 µm; (c–h) 50 µm.

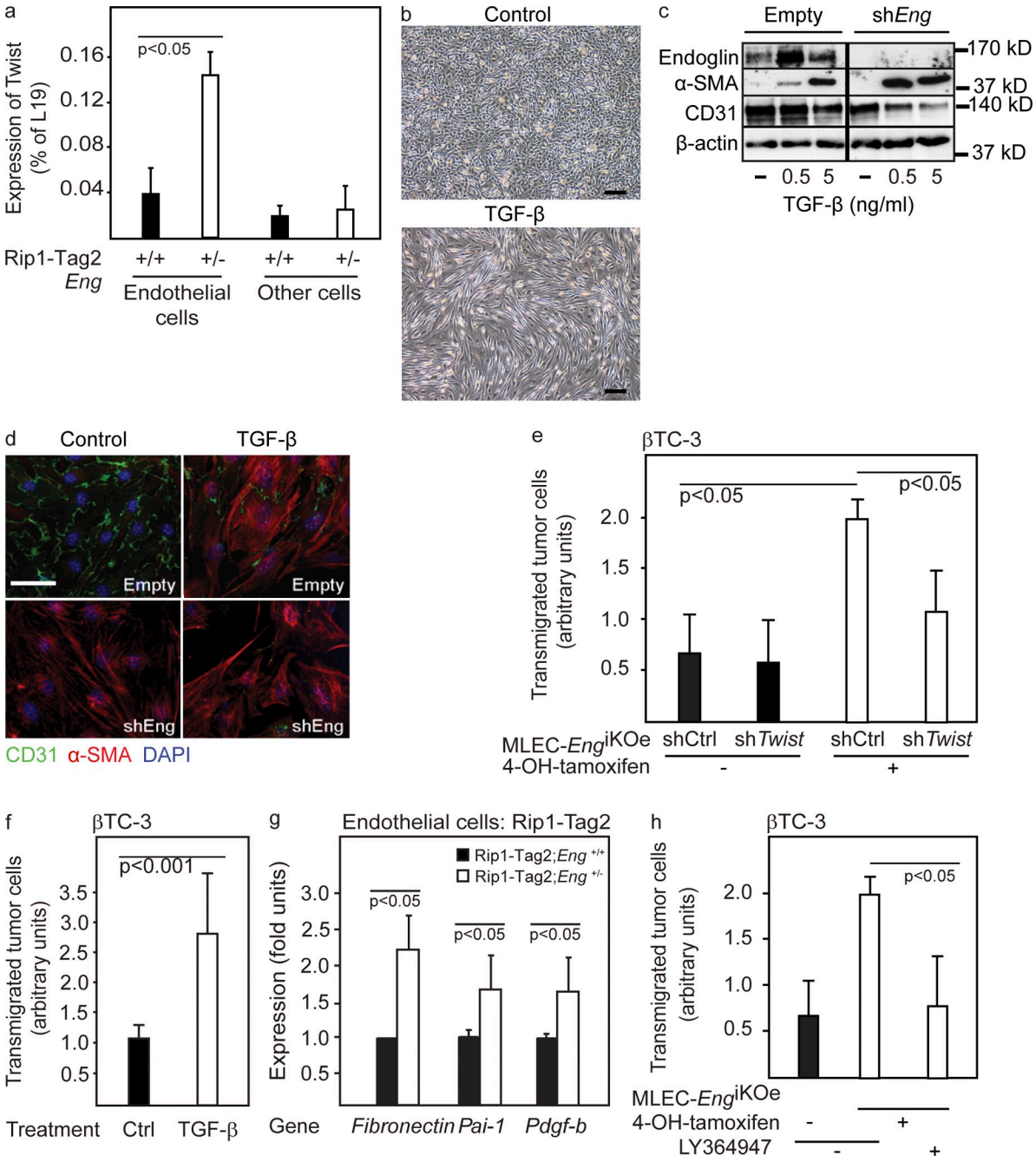

Figure 7. Reduced expression of endoglin in endothelial cells facilitates EndMT and tumor cell transmigration. (a) Quantitative RT-PCR for Twist in isolated endothelial cells or nonendothelial cells (other cells) from PNETs of 12-wk-old RIP1-Tag2;*Eng*$^{+/+}$ and RIP1-Tag2;*Eng*$^{+/-}$ mice. A representative experiment using a pool of material derived from more than six mice per group is shown. (b) Micrograph of bEnd3.1 endothelial cells stimulated with TGF-β for 48 h. (c) Western blot of endoglin, α-SMA, and CD31 in bEnd3.1 cells expressing either shRNA-endoglin or empty vector stimulated with TGF-β. β-Actin served as a loading control. The dividing line marks duplicate lanes that were removed. (d) Immunostaining for CD31 and α-SMA of bEnd3.1/shRNA-endoglin or control cells with and without TGF-β stimulation. (e) Transmigration of βTC-3 cells through a monolayer of MLEC either induced or noninduced to knock out the gene for endoglin by treatment with 4-OH-tamoxifen and infected with a lentiviral control construct (shCtrl) or shTwist construct. The mean of two independent experiments is shown. (f) Transmigration of βTC-3 cells through a monolayer of MS1 pancreatic islet endothelial cells stimulated with TGF-β. The mean of three independent experiments is shown. (g) Quantitative RT-PCR for the ALK5 target genes fibronectin (Fn), plasminogen activator inhibitor-1 (PAI-1), and platelet-derived growth factor B (PDGF-B). A pool of endothelial cell–specific genes (VE-cadherin, CD31, and VEGFR-2) was used as a reference. The mean of two independent experiments is shown (a pool of material derived from more than six mice per group was used for the analysis). (h) Transmigration of β-TC3 cells through a monolayer of MLEC either induced or noninduced to knock out the gene for endoglin by treatment with 4-OH-tamoxifen and in the presence of 1 µM of the ALK5 inhibitor LY364947. The mean of two independent experiments is shown. Error bars depict SD. Bars: (b) 50 µm; (d) 20 µm.

evident under these conditions. Although the loss of endothelial cell identity through down-regulation of endoglin and CD31 correlated with an increased leniency toward tumor cell transmigration, the rate of vascular perfusion or the extent of leakage of molecular tracers into the tumor parenchyma was not altered, in contrast to a recent study demonstrating enhanced vascular permeability in the colon of $Eng^{+/-}$ mice as a result of increased secretion of VEGF (Jerkic et al., 2010). Collectively with the fact that the ultrastructure of endoglin-deficient tumor capillaries was seemingly normal, our findings suggest that tumor cells transmigrate across the endothelium through a controlled process and not simply by using physical gaps in the abnormal tumor vasculature, a conclusion which raises the possibility of developing antimetastatic drugs that interfere with tumor cell intra- and extravasation. Future studies should address whether tumor cells use similar mechanisms for endothelial transmigration as immune cells and whether endothelial cells having undergone EndMT are also more permissive to inflammatory cell transmigration. Indeed, mice deficient for CD31 exhibit a facilitated transendothelial migration of immune cells, and engagement of CD31 on endothelial cells inhibits ICAM-1–induced cytoskeletal rearrangements associated with immune cell trafficking (Graesser et al., 2002; Couty et al., 2007).

Apart from inducing EndMT, TGF-β exerts a wide variety of effects on endothelial cells depending on the molecular context (Pardali et al., 2010; Cunha and Pietras, 2011). Recent work demonstrates that genetic or pharmacological blockade of the endothelial cell–restricted TGF-β type I receptor ALK1 inhibits tumor angiogenesis and growth (Cunha et al., 2010; Mitchell et al., 2010; Hu-Lowe et al., 2011). No overt resistance to the blockade of ALK1 was reported in these studies, but long-term investigations are warranted to make conclusive statements. Targeting of endoglin by genetic, pharmacological, or immunological means consistently diminishes tumor angiogenesis, thereby delaying tumor growth in a range of subcutaneously injected models (Seon et al., 2011). Moreover, high expression of endoglin in the tumor microvasculature, as judged by immunostaining, is associated with a poor patient outcome in different malignancies. As a result of these findings, the human chimeric antibody TRC105 against endoglin is currently being clinically developed. Despite being an attractive and preclinically proven drug target for antiangiogenic therapy of tumors, our data indicate that long-term therapeutic protocols involving pharmacological inhibition of endoglin should be approached with caution (although we acknowledge the potential pitfalls in translating genetic studies into conclusions about pharmacological interventions). In support of this proposition, and as a human correlate to our findings, high serum levels of a soluble form of endoglin, ostensibly an inhibitor of endoglin action, produced by the release of the extracellular domain through cleavage by matrix metalloprotease-14 (Hawinkels et al., 2010), is correlated to the occurrence of metastatic disease in breast and colon carcinoma patients (Takahashi et al., 2001b).

It is interesting to note that genetic loss of a single copy of the gene encoding endoglin was sufficient to induce evasive mechanisms to circumvent the impairment in angiogenesis and cause increased metastatic spread. Thus, one may speculate that cancer patients harboring germline-transmitted hypomorphic alleles of prototypical angiogenic regulators may be predisposed to developing metastatic disease by induction of tumor cell autonomous and/or nonautonomous evasive programs to the genetically impaired angiogenic response. Efforts to identify such high-risk patient groups are highly warranted. Likewise, the observed breakdown of the endothelial barrier to metastatic spread in mice lacking one copy of the endoglin gene holds significance for patients suffering from the syndrome HHT-1, caused by functional heterozygosity for endoglin. Epidemiological studies of the prevalence and prognosis of cancer for HHT-1 patients are difficult to perform as a result of the low incidence in the population. However, special care should be taken to follow up HHT-1 patients afflicted by malignant disease, as our study indicates that their prognosis may be comparatively poor. Interestingly, HHT patients are reported to exhibit increased serum levels of VEGF-A (Sadick et al., 2005, 2008). Collectively with the synergistic interaction of VEGF inhibition and endoglin deficiency observed in the present study, this suggests that tumors of HHT-1 patients may be exquisitely sensitive to drugs incorporating inhibitory action against VEGFRs. Although solitary blockade of angiogenic drivers through targeting of VEGF or endoglin ultimately may lead to therapeutic refractoriness characterized by increased metastatic spread, concurrent targeting of multiple pathways should offer increased efficacy. Thus, we conclude that combinations or cocktails of drugs impinging on distinct signaling pathways in the angiogenic response may prove to efficiently delay the onset of therapy-induced resistance in cancer.

MATERIALS AND METHODS

RNA isolation and quantitative RT-PCR. Total RNA was isolated using the RNeasy kit (QIAGEN) according to the manufacturer's instructions, followed by cDNA synthesis of total RNA using iScript (Bio-Rad Laboratories). Total RNA from whole blood was purified by the RiboPure-Blood RNA Isolation kit (Ambion). Quantitative PCR was performed using the QuantiMix SYBR green kit (BioTools) on a Rotorgene 6000 (QIAGEN) in triplicates. Total RNA from normal, hyperplastic, angiogenic, and tumorous pancreatic islets was a gift from P. Olsen (Pfizer, La Jolla, CA) and D. Hanahan (École Polytechnique Fédérale de Lausanne, Lausanne, Switzerland). Expression levels were calculated relative to the ribosomal reference gene RPL19 as $100 \times 2^{-\Delta Ct}$. For primer sequences for RPL19, endoglin, PAI-1, PDGFB, CD31, and VE-cadherin, see Cunha et al. (2010); for VEGFR2, see Hagberg et al. (2010); for Twist, see Yang et al. (2004); primers for fibronectin were purchased from QIAGEN (QT00135758); and primers for SV40 T-Ag were 5′-GGAAAGTCCTTGGGGTCTTC-3′ (forward) and 5′-CTGACTTTGGAGGCTTCTGG-3′ (reverse).

Tissue preparation, histology, and immunostaining. Mice were heart perfused with PBS followed by 2% paraformaldehyde. For paraffin embedding, organs were postfixed in 2% paraformaldehyde at 4°C overnight. For cryopreservation, tumors and pancreata were kept in 30% sucrose at 4°C overnight, followed by embedding in cryosectioning media. Frozen sections were fixed in cold acetone, followed by blocking using serum-free protein block

(DAKO) or 0.5% blocking reagent in PBS (NEN Life Science Products) for >90 min at room temperature. Primary antibodies directed against CD31 (clone 2H8; dilution 1:200; Millipore), Endoglin (clone MJ7/18; dilution 1:100 to 1:200; eBioscience), Podocalyxin (dilution 1:100; AF1556; R&D Systems), CD31 (MEC13.3; dilution 1:100 or 1:25 for LLC-RFP tumors; BD), α-SMA–Cy3 (clone 1A4; dilution 1:100; Sigma-Aldrich), and NG2 (AB5320; dilution 1:400; Millipore) were incubated overnight at 4°C. Appropriate fluorochrome-conjugated secondary antibodies (Invitrogen) were used and sections were mounted using mounting media containing 4′,6-diamidino-2-phenylindole (Vector Laboratories). Imaging was performed using a microscope (Eclipse E800; Nikon) equipped with Plan Fluor objectives (10×, NA 0.30; 20×, NA 0.50; 40×, NA 0.75) at room temperature in air using Alexa Fluor 594– and Alexa Fluor 488–coupled secondary antibodies. Images were acquired using a SPOT RTKE camera using the SPOT advanced software. For ultrastructural analysis, PNETs were fixed in 2% paraformaldehyde and 2.5% glutaraldehyde followed by ferrocyanide-reduced osmium tetroxide. After uranyl staining en bloc, specimens were dehydrated and embedded in epoxy resin according to standard routines. Ultrathin sections were examined in an electron microscope (LEO 912AB; Omega) equipped with a camera (SiS Veleta; Olympus) under iTEM software control.

Animal care and tumor establishment. All animal experiments were approved by the local committees for animal care (Stockholm, Sweden and Newcastle, UK). Angiogenic islets from RIP1-Tag2 mice were defined as overtly red islets <1 × 1 mm, as assessed under a stereological microscope. *Eng*-iKO^{e} mice and control mice were generated as previously described (Mahmoud et al., 2010). To establish EO771 tumors, 5×10^5 cells were injected orthopically into the fourth mammary fat pad of young $Eng^{+/+}$ or $Eng^{+/-}$ females. Anesthetized 8–12-wk-old female mice were injected with 2.5×10^6 LLC-RFP cells subdermally. Tumor volume was calculated as length × width^2 × π/6.

Quantification of vascular parameters. Perfused vessels were assessed after 4 min of circulation of 50 µl of 0.5 mg/ml fluorescein-conjugated tomato lectin (Vector Laboratories) injected retroorbitally. Vessel density and perfusion was analyzed using Photoshop (Adobe), Volocity (PerkinElmer), or ImageJ (National Institutes of Health) software and quantified as number of positively stained pixels per area. The abundance of cells expressing mural cell markers was quantified as the number of positively stained pixels adjusted for vascular density. For each analysis, >10 images/mouse were used.

Cell culture. βTC-3 and LLC-RFP cells (a gift from V. Mittal, Weill Cornell Medical College, New York, NY) were maintained in RPMI and DMEM (Invitrogen), respectively, supplemented with 10% FCS. EO771 cells (a gift from R. Ray, Saint Louis University School of Medicine, St. Louis, MO) were cultured in DMEM low glucose supplemented with 20% FCS. MS1 and bEND3.1 cells were cultured in Endothelial Cell Basal Medium MV2 kit (PromoCell). Primary endothelial cells from Eng^{iKOe} mice carrying the Immortomouse transgene were isolated from the lung (MLEC) and propagated in endothelial cell medium containing 20 U/ml recombinant mouse interferon-γ (PeproTech) at 33°C. All experiments using MLEC were performed at 37°C. Induction of knockout of the endoglin gene was achieved by growing MLEC in endothelial cell medium containing 1 µM 4-OH-tamoxifen (Sigma-Aldrich) for 48 h. Expression of endoglin, Twist, and CD31 was stably knocked down in endothelial cells by lentivirally transduced shRNA-containing vectors (Santa Cruz Biotechnology, Inc.).

Quantification of metastases and tumor cell extravasation. The right lateral liver lobe and the superior and middle lung lobe from the RIP1-Tag2 mice and EO771 tumor model, respectively, were paraffin embedded and sectioned in their entirety. To analyze tumor cell extravasation, 10^6 fluorescently labeled (Vybrant CFDA SE Cell Tracer kit; Invitrogen) βTC-3 cells were injected into the tail vein and allowed to circulate for 24 h, after which the right lateral liver lobe was embedded and sectioned, and 30 consecutive sections were examined for extravasated labeled βTC-3 cells. Lungs from the LLC-RFP tumor model were removed for analysis of metastases with a fluorescence stereomicroscope at 18 d after subdermal inoculation or 15 d after tail vein injection of 2.5×10^5 LLC-RFP cells to examine extravasation.

Therapeutic trials. AG-028262 (a gift from D. Hu-Lowe, Pfizer) was dissolved in 0.5% carboxymethylcellulose and was administered at a dose of 75 mg/kg once daily by oral gavage. The effective dose of AG-028262 was 54.8 mg/kg after correction for the fraction of active drug contained in the particular batch used (73.1% active compound). DC101 was delivered intraperitoneally twice weekly at 1 mg/mouse and injection. RIP1-Tag2;$Eng^{+/+}$ and RIP1-Tag2;$Eng^{+/-}$ mice were treated with vehicle, AG-028262, or DC101 from 10 wk of age for 3 wk. Mice carrying EO771 tumors were treated with AG-028262 or vehicle for 2 wk starting 7 d after establishment.

Tumor cell transmigration assay. 60,000 bEND.3 cells or 75.000 MS1 cells were seeded in 8-µm pore inserts and allowed to form a monolayer. βTC-3 or EO771 cells were labeled in green using the Vybrant CFDA SE Cell Tracer kit (Invitrogen), and 500,000 labeled tumor cells were seeded over the endothelial cell monolayer and allowed to transmigrate for 24 h. The inserts were fixed, cut, and mounted on a slide with DAPI-containing mounting medium. The transmigration index was assessed by quantifying 10–12 high-power fields per insert and was expressed as the percentage of green-positive pixels per total number of DAPI-positive pixels.

Endothelial cell isolation. RIP1-Tag2 mice (more than six mice per isolation) were heart perfused with PBS, and tumors were dissected and minced and digested in 0.05 g collagenase type II (Worthington), 0.05 g collagenase IV (Invitrogen), and 0.01 g DNase I (Sigma-Aldrich) for 15 min at 37°C with vigorous stirring. After passing tissue through a 70-µm strainer, the solution was centrifuged at 1.2 krpm at 4°C for 8 min. The pellet was dissolved in 10 ml PharmLyse buffer for 10 min at room temperature, resuspended in 1 ml buffer and 50 µl CD31-coated beads (Biotin-conjugated MEC13.3 CD31 antibody [BD] and CELLection biotin binder kit [Invitrogen]), and incubated end over end at 4°C for 30 min. Using a magnetic bead collector, beads were washed eight times. Supernatant from the first collection was designated the other cell fraction. Using quantitative RT-PCR, an endothelial cell enrichment index was calculated by correlating the relative abundance of the endothelial cell markers CD31, VE-cadherin, and VEGFR-2 for each preparation.

Statistical analysis. Unless specifically stated to the contrary, all measurements are depicted as mean ± SD. Statistical analyses were, unless otherwise noted, performed using an unpaired two-tailed Student's *t* test. Statistical analysis of the frequency of angiogenic islets or tumor-free mice was performed using a χ^2-test. Statistical significance was considered using $\alpha = 0.05$.

We thank Douglas Hanahan and Peter Olsen for providing RNA from different stages of PNET development; Vivek Mittal and Ratna Ray for providing LLC-RFP and EO771 cells, respectively; Dana Hu-Lowe and Pfizer for providing AG-028262; and Ingrid Nilsson, Stephen Smith, and Neil Hamilton for technical assistance.

K. Pietras is the Göran and Birgitta Grosskopf Professor of Molecular Medicine and the recipient of Young Investigator Awards from the Swedish Cancer Society and StratCan. This work was supported by the ERC Starting grant TUMORGAN, as well as grants to K. Pietras from the Swedish Cancer Society, the Swedish Research Council (project# K2011-67X-21865-01-6), the Swedish Childhood Cancer Society, Jeansson's Foundation, Magn Bergvalls Foundation, Åke Wiberg's Foundation, BioCARE, and Lund University. In addition, support was provided by a Linnaeus grant to the STARGET consortium from the Swedish Research Council and by strategic funds to the BRECT network. H.M. Arthur is supported by a BHF senior basic science research fellowship, and the work was supported by a project grant form CRUK. P. ten Dijke is supported by the Dutch Cancer Society.

The authors have no financial conflicts of interest.

Submitted: 26 March 2012
Accepted: 17 January 2013

REFERENCES

Arthur, H.M., J. Ure, A.J. Smith, G. Renforth, D.I. Wilson, E. Torsney, R. Charlton, D.V. Parums, T. Jowett, D.A. Marchuk, et al. 2000. Endoglin, an ancillary TGFbeta receptor, is required for extraembryonic angiogenesis and plays a key role in heart development. *Dev. Biol.* 217:42–53. http://dx.doi.org/10.1006/dbio.1999.9534

Bergers, G., and D. Hanahan. 2008. Modes of resistance to anti-angiogenic therapy. *Nat. Rev. Cancer.* 8:592–603. http://dx.doi.org/10.1038/nrc2442

Bernabeu, C., J.M. Lopez-Novoa, and M. Quintanilla. 2009. The emerging role of TGF-beta superfamily coreceptors in cancer. *Biochim. Biophys. Acta.* 1792:954–973. http://dx.doi.org/10.1016/j.bbadis.2009.07.003

Blanco, F.J., J.F. Santibanez, M. Guerrero-Esteo, C. Langa, C.P. Vary, and C. Bernabeu. 2005. Interaction and functional interplay between endoglin and ALK-1, two components of the endothelial transforming growth factor-beta receptor complex. *J. Cell. Physiol.* 204:574–584. http://dx.doi.org/10.1002/jcp.20311

Bourdeau, A., D.J. Dumont, and M. Letarte. 1999. A murine model of hereditary hemorrhagic telangiectasia. *J. Clin. Invest.* 104:1343–1351. http://dx.doi.org/10.1172/JCI8088

Burrows, F.J., E.J. Derbyshire, P.L. Tazzari, P. Amlot, A.F. Gazdar, S.W. King, M. Letarte, E.S. Vitetta, and P.E. Thorpe. 1995. Up-regulation of endoglin on vascular endothelial cells in human solid tumors: implications for diagnosis and therapy. *Clin. Cancer Res.* 1:1623–1634.

Casanovas, O., D.J. Hicklin, G. Bergers, and D. Hanahan. 2005. Drug resistance by evasion of antiangiogenic targeting of VEGF signaling in late-stage pancreatic islet tumors. *Cancer Cell.* 8:299–309. http://dx.doi.org/10.1016/j.ccr.2005.09.005

Casey, A.E., W.R. Laster Jr., and G.L. Ross. 1951. Sustained enhanced growth of carcinoma EO771 in C57 black mice. *Proc. Soc. Exp. Biol. Med.* 77:358–362.

Castonguay, R., E.D. Werner, R.G. Matthews, E. Presman, A.W. Mulivor, N. Solban, D. Sako, R.S. Pearsall, K.W. Underwood, J. Seehra, et al. 2011. Soluble endoglin specifically binds bone morphogenetic proteins 9 and 10 via its orphan domain, inhibits blood vessel formation, and suppresses tumor growth. *J. Biol. Chem.* 286:30034–30046. http://dx.doi.org/10.1074/jbc.M111.260133

Charpin, C., J.P. Dales, S. Garcia, S. Carpentier, A. Djemli, L. Andrac, M.N. Lavaut, C. Allasia, and P. Bonnier. 2004. Tumor neoangiogenesis by CD31 and CD105 expression evaluation in breast carcinoma tissue microarrays. *Clin. Cancer Res.* 10:5815–5819. http://dx.doi.org/10.1158/1078-0432.CCR-04-0021

Chiu, C.W., H. Nozawa, and D. Hanahan. 2010. Survival benefit with proapoptotic molecular and pathologic responses from dual targeting of mammalian target of rapamycin and epidermal growth factor receptor in a preclinical model of pancreatic neuroendocrine carcinogenesis. *J. Clin. Oncol.* 28:4425–4433. http://dx.doi.org/10.1200/JCO.2010.28.0198

Chung, A.S., M. Kowanetz, X. Wu, G. Zhuang, H. Ngu, D. Finkle, L. Komuves, F. Peale, and N. Ferrara. 2012. Differential drug class-specific metastatic effects following treatment with a panel of angiogenesis inhibitors. *J. Pathol.* 227:404–416. http://dx.doi.org/10.1002/path.4052

Couty, J.P., C. Rampon, M. Leveque, M.P. Laran-Chich, S. Bourdoulous, J. Greenwood, and P.O. Couraud. 2007. PECAM-1 engagement counteracts ICAM-1-induced signaling in brain vascular endothelial cells. *J. Neurochem.* 103:793–801. http://dx.doi.org/10.1111/j.1471-4159.2007.04782.x

Cunha, S.I., and K. Pietras. 2011. ALK1 as an emerging target for antiangiogenic therapy of cancer. *Blood.* 117:6999–7006. http://dx.doi.org/10.1182/blood-2011-01-330142

Cunha, S.I., E. Pardali, M. Thorikay, C. Anderberg, L. Hawinkels, M.J. Goumans, J. Seehra, C.H. Heldin, P. ten Dijke, and K. Pietras. 2010. Genetic and pharmacological targeting of activin receptor-like kinase 1 impairs tumor growth and angiogenesis. *J. Exp. Med.* 207:85–100. http://dx.doi.org/10.1084/jem.20091309

Dales, J.P., S. Garcia, L. Andrac, S. Carpentier, O. Ramuz, M.N. Lavaut, C. Allasia, P. Bonnier, and C. Charpin. 2004. Prognostic significance of angiogenesis evaluated by CD105 expression compared to CD31 in 905 breast carcinomas: correlation with long-term patient outcome. *Int. J. Oncol.* 24:1197–1204.

David, L., J.J. Feige, and S. Bailly. 2009. Emerging role of bone morphogenetic proteins in angiogenesis. *Cytokine Growth Factor Rev.* 20:203–212. http://dx.doi.org/10.1016/j.cytogfr.2009.05.001

Düwel, A., N. Eleno, M. Jerkic, M. Arevalo, J.P. Bolaños, C. Bernabeu, and J.M. López-Novoa. 2007. Reduced tumor growth and angiogenesis in endoglin-haploinsufficient mice. *Tumour Biol.* 28:1–8.

Ebos, J.M., C.R. Lee, W. Cruz-Munoz, G.A. Bjarnason, J.G. Christensen, and R.S. Kerbel. 2009a. Accelerated metastasis after short-term treatment with a potent inhibitor of tumor angiogenesis. *Cancer Cell.* 15:232–239. http://dx.doi.org/10.1016/j.ccr.2009.01.021

Ebos, J.M., C.R. Lee, and R.S. Kerbel. 2009b. Tumor and host-mediated pathways of resistance and disease progression in response to antiangiogenic therapy. *Clin. Cancer Res.* 15:5020–5025. http://dx.doi.org/10.1158/1078-0432.CCR-09-0095

Efrat, S., S. Linde, H. Kofod, D. Spector, M. Delannoy, S. Grant, D. Hanahan, and S. Baekkeskov. 1988. Beta-cell lines derived from transgenic mice expressing a hybrid insulin gene-oncogene. *Proc. Natl. Acad. Sci. USA.* 85:9037–9041. http://dx.doi.org/10.1073/pnas.85.23.9037

Egorova, A.D., P.P. Khedoe, M.J. Goumans, B.K. Yoder, S.M. Nauli, P. ten Dijke, R.E. Poelmann, and B.P. Hierck. 2011. Lack of primary cilia primes shear-induced endothelial-to-mesenchymal transition. *Circ. Res.* 108:1093–1101. http://dx.doi.org/10.1161/CIRCRESAHA.110.231860

Escudier, B., T. Eisen, W.M. Stadler, C. Szczylik, S. Oudard, M. Siebels, S. Negrier, C. Chevreau, E. Solska, A.A. Desai, et al; TARGET Study Group. 2007. Sorafenib in advanced clear-cell renal-cell carcinoma. *N. Engl. J. Med.* 356:125–134. http://dx.doi.org/10.1056/NEJMoa060655

Franco, M., M. Pàez-Ribes, E. Cortez, O. Casanovas, and K. Pietras. 2011a. Use of a mouse model of pancreatic neuroendocrine tumors to find pericyte biomarkers of resistance to anti-angiogenic therapy. *Horm. Metab. Res.* 43:884–889. http://dx.doi.org/10.1055/s-0031-1284381

Franco, M., P. Roswall, E. Cortez, D. Hanahan, and K. Pietras. 2011b. Pericytes promote endothelial cell survival through induction of autocrine VEGF-A signaling and Bcl-w expression. *Blood.* 118:2906–2917. http://dx.doi.org/10.1182/blood-2011-01-331694

Graesser, D., A. Solowiej, M. Bruckner, E. Osterweil, A. Juedes, S. Davis, N.H. Ruddle, B. Engelhardt, and J.A. Madri. 2002. Altered vascular permeability and early onset of experimental autoimmune encephalomyelitis in PECAM-1-deficient mice. *J. Clin. Invest.* 109:383–392.

Hagberg, C.E., A. Falkevall, X. Wang, E. Larsson, J. Huusko, I. Nilsson, L.A. van Meeteren, E. Samen, L. Lu, M. Vanwildemeersch, et al. 2010. Vascular endothelial growth factor B controls endothelial fatty acid uptake. *Nature.* 464:917–921. http://dx.doi.org/10.1038/nature08945

Hanahan, D. 1985. Heritable formation of pancreatic beta-cell tumours in transgenic mice expressing recombinant insulin/simian virus 40 oncogenes. *Nature.* 315:115–122. http://dx.doi.org/10.1038/315115a0

Hawinkels, L.J., P. Kuiper, E. Wiercinska, H.W. Verspaget, Z. Liu, E. Pardali, C.F. Sier, and P. ten Dijke. 2010. Matrix metalloproteinase-14 (MT1-MMP)-mediated endoglin shedding inhibits tumor angiogenesis. *Cancer Res.* 70:4141–4150. http://dx.doi.org/10.1158/0008-5472.CAN-09-4466

Helfrich, I., I. Scheffrahn, S. Bartling, J. Weis, V. von Felbert, M. Middleton, M. Kato, S. Ergün, and D. Schadendorf. 2010. Resistance to antiangiogenic therapy is directed by vascular phenotype, vessel stabilization, and maturation in malignant melanoma. *J. Exp. Med.* 207:491–503. http://dx.doi.org/10.1084/jem.20091846

Horvat, R., A. Hovorka, G. Dekan, H. Poczewski, and D. Kerjaschki. 1986. Endothelial cell membranes contain podocalyxin—the major sialoprotein of visceral glomerular epithelial cells. *J. Cell Biol.* 102:484–491. http://dx.doi.org/10.1083/jcb.102.2.484

Hu-Lowe, D.D., E. Chen, L. Zhang, K.D. Watson, P. Mancuso, P. Lappin, G. Wickman, J.H. Chen, J. Wang, X. Jiang, et al. 2011. Targeting activin receptor-like kinase 1 inhibits angiogenesis and tumorigenesis through a mechanism of action complementary to anti-VEGF therapies. *Cancer Res.* 71:1362–1373. http://dx.doi.org/10.1158/0008-5472.CAN-10-1451

Hurwitz, H., L. Fehrenbacher, W. Novotny, T. Cartwright, J. Hainsworth, W. Heim, J. Berlin, A. Baron, S. Griffing, E. Holmgren, et al. 2004.

Bevacizumab plus irinotecan, fluorouracil, and leucovorin for metastatic colorectal cancer. *N. Engl. J. Med.* 350:2335–2342. http://dx.doi.org/10.1056/NEJMoa032691

Jerkic, M., A. Rodríguez-Barbero, M. Prieto, M. Toporsian, M. Pericacho, J.V. Rivas-Elena, J. Obreo, A. Wang, F. Pérez-Barriocanal, M. Arévalo, et al. 2006. Reduced angiogenic responses in adult Endoglin heterozygous mice. *Cardiovasc. Res.* 69:845–854. http://dx.doi.org/10.1016/j.cardiores.2005.11.020

Jerkic, M., M. Peter, D. Ardelean, M. Fine, M.A. Konerding, and M. Letarte. 2010. Dextran sulfate sodium leads to chronic colitis and pathological angiogenesis in Endoglin heterozygous mice. *Inflamm. Bowel Dis.* 16:1859–1870. http://dx.doi.org/10.1002/ibd.21288

Jonker, L., and H.M. Arthur. 2002. Endoglin expression in early development is associated with vasculogenesis and angiogenesis. *Mech. Dev.* 110:193–196. http://dx.doi.org/10.1016/S0925-4773(01)00562-7

Kerbel, R.S. 1991. Inhibition of tumor angiogenesis as a strategy to circumvent acquired resistance to anti-cancer therapeutic agents. *Bioessays.* 13:31–36. http://dx.doi.org/10.1002/bies.950130106

Kerbel, R.S. 1997. A cancer therapy resistant to resistance. *Nature.* 390:335–336. http://dx.doi.org/10.1038/36978

Kumar, S., A. Ghellal, C. Li, G. Byrne, N. Haboubi, J.M. Wang, and N. Bundred. 1999. Breast carcinoma: vascular density determined using CD105 antibody correlates with tumor prognosis. *Cancer Res.* 59:856–861.

Lebrin, F., M.J. Goumans, L. Jonker, R.L. Carvalho, G. Valdimarsdottir, M. Thorikay, C. Mummery, H.M. Arthur, and P. ten Dijke. 2004. Endoglin promotes endothelial cell proliferation and TGF-beta/ALK1 signal transduction. *EMBO J.* 23:4018–4028. http://dx.doi.org/10.1038/sj.emboj.7600386

Li, D.Y., L.K. Sorensen, B.S. Brooke, L.D. Urness, E.C. Davis, D.G. Taylor, B.B. Boak, and D.P. Wendel. 1999. Defective angiogenesis in mice lacking endoglin. *Science.* 284:1534–1537. http://dx.doi.org/10.1126/science.284.5419.1534

Mahmoud, M., K.R. Allinson, Z. Zhai, R. Oakenfull, P. Ghandi, R.H. Adams, M. Fruttiger, and H.M. Arthur. 2010. Pathogenesis of arteriovenous malformations in the absence of endoglin. *Circ. Res.* 106:1425–1433. http://dx.doi.org/10.1161/CIRCRESAHA.109.211037

Martone, T., P. Rosso, R. Albera, G. Migliaretti, F. Fraire, L. Pignataro, G. Pruneri, G. Bellone, and G. Cortesina. 2005. Prognostic relevance of CD105+ microvessel density in HNSCC patient outcome. *Oral Oncol.* 41:147–155. http://dx.doi.org/10.1016/j.oraloncology.2004.08.001

Massagué, J. 2008. TGFbeta in Cancer. *Cell.* 134:215–230. http://dx.doi.org/10.1016/j.cell.2008.07.001

Medici, D., E.M. Shore, V.Y. Lounev, F.S. Kaplan, R. Kalluri, and B.R. Olsen. 2010. Conversion of vascular endothelial cells into multipotent stem-like cells. *Nat. Med.* 16:1400–1406. http://dx.doi.org/10.1038/nm.2252

Miller, D.W., W. Graulich, B. Karges, S. Stahl, M. Ernst, A. Ramaswamy, H.H. Sedlacek, R. Müller, and J. Adamkiewicz. 1999. Elevated expression of endoglin, a component of the TGF-beta-receptor complex, correlates with proliferation of tumor endothelial cells. *Int. J. Cancer.* 81:568–572. http://dx.doi.org/10.1002/(SICI)1097-0215(19990517)81:4<568::AID-IJC11>3.0.CO;2-X

Mitchell, D., E.G. Pobre, A.W. Mulivor, A.V. Grinberg, R. Castonguay, T.E. Monnell, N. Solban, J.A. Ucran, R.S. Pearsall, K.W. Underwood, et al. 2010. ALK1-Fc inhibits multiple mediators of angiogenesis and suppresses tumor growth. *Mol. Cancer Ther.* 9:379–388. http://dx.doi.org/10.1158/1535-7163.MCT-09-0650

Moonen, J.R., G. Krenning, M.G. Brinker, J.A. Koerts, M.J. van Luyn, and M.C. Harmsen. 2010. Endothelial progenitor cells give rise to pro-angiogenic smooth muscle-like progeny. *Cardiovasc. Res.* 86:506–515. http://dx.doi.org/10.1093/cvr/cvq012

Motzer, R.J., T.E. Hutson, P. Tomczak, M.D. Michaelson, R.M. Bukowski, O. Rixe, S. Oudard, S. Negrier, C. Szczylik, S.T. Kim, et al. 2007. Sunitinib versus interferon alfa in metastatic renal-cell carcinoma. *N. Engl. J. Med.* 356:115–124. http://dx.doi.org/10.1056/NEJMoa065044

Nassiri, F., M.D. Cusimano, B.W. Scheithauer, F. Rotondo, A. Fazio, G.M. Yousef, L.V. Syro, K. Kovacs, and R.V. Lloyd. 2011. Endoglin (CD105): a review of its role in angiogenesis and tumor diagnosis, progression and therapy. *Anticancer Res.* 31:2283–2290.

Nguyen, D.X., P.D. Bos, and J. Massagué. 2009. Metastasis: from dissemination to organ-specific colonization. *Nat. Rev. Cancer.* 9:274–284. http://dx.doi.org/10.1038/nrc2622

Padua, D., and J. Massagué. 2009. Roles of TGFbeta in metastasis. *Cell Res.* 19:89–102. http://dx.doi.org/10.1038/cr.2008.316

Pàez-Ribes, M., E. Allen, J. Hudock, T. Takeda, H. Okuyama, F. Viñals, M. Inoue, G. Bergers, D. Hanahan, and O. Casanovas. 2009. Antiangiogenic therapy elicits malignant progression of tumors to increased local invasion and distant metastasis. *Cancer Cell.* 15:220–231. http://dx.doi.org/10.1016/j.ccr.2009.01.027

Pardali, E., M.J. Goumans, and P. ten Dijke. 2010. Signaling by members of the TGF-beta family in vascular morphogenesis and disease. *Trends Cell Biol.* 20:556–567. http://dx.doi.org/10.1016/j.tcb.2010.06.006

Pavel, M., E. Baudin, A. Couvelard, E. Krenning, K. Öberg, T. Steinmüller, M. Anlauf, B. Wiedenmann, and R. Salazar; Barcelona Consensus Conference participants. 2012. ENETS Consensus Guidelines for the management of patients with liver and other distant metastases from neuroendocrine neoplasms of foregut, midgut, hindgut, and unknown primary. *Neuroendocrinology.* 95:157–176. http://dx.doi.org/10.1159/000335597

Pérez-Gómez, E., G. Del Castillo, S. Juan Francisco, J.M. López-Novoa, C. Bernabéu, and M. Quintanilla. 2010. The role of the TGF-β coreceptor endoglin in cancer. *ScientificWorldJournal.* 10:2367–2384. http://dx.doi.org/10.1100/tsw.2010.230

Pietras, K., and D. Hanahan. 2005. A multitargeted, metronomic, and maximum-tolerated dose "chemo-switch" regimen is antiangiogenic, producing objective responses and survival benefit in a mouse model of cancer. *J. Clin. Oncol.* 23:939–952. http://dx.doi.org/10.1200/JCO.2005.07.093

Raymond, E., L. Dahan, J.L. Raoul, Y.J. Bang, I. Borbath, C. Lombard-Bohas, J. Valle, P. Metrakos, D. Smith, A. Vinik, et al. 2011. Sunitinib malate for the treatment of pancreatic neuroendocrine tumors. *N. Engl. J. Med.* 364:501–513. http://dx.doi.org/10.1056/NEJMoa1003825

Sadick, H., F. Riedel, R. Naim, U. Goessler, K. Hörmann, M. Hafner, and A. Lux. 2005. Patients with hereditary hemorrhagic telangiectasia have increased plasma levels of vascular endothelial growth factor and transforming growth factor-beta1 as well as high ALK1 tissue expression. *Haematologica.* 90:818–828.

Sadick, H., J. Hage, U. Goessler, G. Bran, F. Riedel, P. Bugert, and K. Hoermann. 2008. Does the genotype of HHT patients with mutations of the ENG and ACVRL1 gene correlate to different expression levels of the angiogenic factor VEGF? *Int. J. Mol. Med.* 22:575–580.

Seon, B.K., F. Matsuno, Y. Haruta, M. Kondo, and M. Barcos. 1997. Long-lasting complete inhibition of human solid tumors in SCID mice by targeting endothelial cells of tumor vasculature with antihuman endoglin immunotoxin. *Clin. Cancer Res.* 3:1031–1044.

Seon, B.K., A. Haba, F. Matsuno, N. Takahashi, M. Tsujie, X. She, N. Harada, S. Uneda, T. Tsujie, H. Toi, et al. 2011. Endoglin-targeted cancer therapy. *Curr. Drug Deliv.* 8:135–143. http://dx.doi.org/10.2174/156720111793663570

Shovlin, C.L. 2010. Hereditary haemorrhagic telangiectasia: pathophysiology, diagnosis and treatment. *Blood Rev.* 24:203–219. http://dx.doi.org/10.1016/j.blre.2010.07.001

Singh, M., S.S. Couto, W.F. Forrest, A. Lima, J.H. Cheng, R. Molina, J.E. Long, P. Hamilton, A. McNutt, I. Kasman, et al. 2012. Anti-VEGF antibody therapy does not promote metastasis in genetically engineered mouse tumour models. *J. Pathol.* 227:417–430. http://dx.doi.org/10.1002/path.4053

Takahashi, N., A. Haba, F. Matsuno, and B.K. Seon. 2001a. Antiangiogenic therapy of established tumors in human skin/severe combined immunodeficiency mouse chimeras by anti-endoglin (CD105) monoclonal antibodies, and synergy between anti-endoglin antibody and cyclophosphamide. *Cancer Res.* 61:7846–7854.

Takahashi, N., R. Kawanishi-Tabata, A. Haba, M. Tabata, Y. Haruta, H. Tsai, and B.K. Seon. 2001b. Association of serum endoglin with metastasis in patients with colorectal, breast, and other solid tumors, and suppressive effect of chemotherapy on the serum endoglin. *Clin. Cancer Res.* 7:524–532.

ten Dijke, P., and H.M. Arthur. 2007. Extracellular control of TGFbeta signalling in vascular development and disease. *Nat. Rev. Mol. Cell Biol.* 8:857–869. http://dx.doi.org/10.1038/nrm2262

ten Dijke, P., M.J. Goumans, and E. Pardali. 2008. Endoglin in angiogenesis and vascular diseases. *Angiogenesis.* 11:79–89. http://dx.doi.org/10.1007/s10456-008-9101-9

Torsney, E., R. Charlton, A.G. Diamond, J. Burn, J.V. Soames, and H.M. Arthur. 2003. Mouse model for hereditary hemorrhagic telangiectasia has a generalized vascular abnormality. *Circulation.* 107:1653–1657. http://dx.doi.org/10.1161/01.CIR.0000058170.92267.00

van Meeteren, L.A., M.J. Goumans, and P. ten Dijke. 2011. TGF-β receptor signaling pathways in angiogenesis; emerging targets for anti-angiogenesis therapy. *Curr. Pharm. Biotechnol.* 12:2108–2120. http://dx.doi.org/10.2174/138920111798808338

Welti, J.C., T. Powles, S. Foo, M. Gourlaouen, N. Preece, J. Foster, S. Frentzas, D. Bird, K. Sharpe, A. van Weverwijk, et al. 2012. Contrasting effects of sunitinib within in vivo models of metastasis. *Angiogenesis.* 15:623–641. http://dx.doi.org/10.1007/s10456-012-9291-z

Westphal, J.R., H.W. Willems, C.J. Schalkwijk, D.J. Ruiter, and R.M. De Waal. 1993. Characteristics and possible function of endoglin, a TGF-beta binding protein. *Behring Inst. Mitt.* 92:15–22.

Wikström, P., I.F. Lissbrant, P. Stattin, L. Egevad, and A. Bergh. 2002. Endoglin (CD105) is expressed on immature blood vessels and is a marker for survival in prostate cancer. *Prostate.* 51:268–275. http://dx.doi.org/10.1002/pros.10083

Xian, X., J. Håkansson, A. Ståhlberg, P. Lindblom, C. Betsholtz, H. Gerhardt, and H. Semb. 2006. Pericytes limit tumor cell metastasis. *J. Clin. Invest.* 116:642–651. http://dx.doi.org/10.1172/JCI25705

Yang, J., S.A. Mani, J.L. Donaher, S. Ramaswamy, R.A. Itzykson, C. Come, P. Savagner, I. Gitelman, A. Richardson, and R.A. Weinberg. 2004. Twist, a master regulator of morphogenesis, plays an essential role in tumor metastasis. *Cell.* 117:927–939. http://dx.doi.org/10.1016/j.cell.2004.06.006

Yao, J.C., M.H. Shah, T. Ito, C.L. Bohas, E.M. Wolin, E. Van Cutsem, T.J. Hobday, T. Okusaka, J. Capdevila, E.G. de Vries, et al; RAD001 in Advanced Neuroendocrine Tumors, Third Trial (RADIANT-3) Study Group. 2011. Everolimus for advanced pancreatic neuroendocrine tumors. *N. Engl. J. Med.* 364:514–523. http://dx.doi.org/10.1056/NEJMoa1009290

Zeisberg, E.M., S. Potenta, L. Xie, M. Zeisberg, and R. Kalluri. 2007. Discovery of endothelial to mesenchymal transition as a source for carcinoma-associated fibroblasts. *Cancer Res.* 67:10123–10128. http://dx.doi.org/10.1158/0008-5472.CAN-07-3127